DIGITAL ACCESS TO SCHOLARSHIP AT HARVARD
DASH.HARVARD.EDU

HARVARD LIBRARY
Office for Scholarly Communication

Changes in Language Pathways in Tuberous Sclerosis Complex Patients with Autism

Citation
Lewis, William. 2014. Changes in Language Pathways in Tuberous Sclerosis Complex Patients with Autism. Doctoral dissertation, Harvard Medical School.

Permanent link
http://nrs.harvard.edu/urn-3:HUL.InstRepos:12407607

Terms of Use
This article was downloaded from Harvard University's DASH repository, and is made available under the terms and conditions applicable to Other Posted Material, as set forth at http://nrs.harvard.edu/urn-3:HUL.InstRepos:dash.current.terms-of-use#LAA

Share Your Story

The Harvard community has made this article openly available.
Please share how this access benefits you. Submit a story .

Accessibility

Table of Contents

Abstract

Tuberous sclerosis complex (TSC) is an autosomal-dominant neurocutaneous disease caused by loss of the *TSC1* (encoding hamartin) or *TSC2* (encoding tuberin) genes. Neurologic symptoms are common and varied in TSC and include epilepsy and behavioral conditions like autism spectrum disorders (ASD). Between 17 and 61% of children with TSC exhibit symptoms of ASD.

The purpose of this study was to investigate a potential correlate of poor neurological outcome in TSC by assessing the integrity of brain language pathways and the relationship to ASD.

42 patients with TSC and 42 age-matched control subjects were scanned with advanced diffusion-weighted MRI. White matter language pathways were identified with a validated automatic method and analyzed for microstructural characteristics, including fractional anisotropy (FA) and mean diffusivity (MD). Well-defined white matter pathways in the brain are characterized by high FA and low MD. During normal development, brain white matter pathways increase in FA and decrease in MD.

Out of 42 patients with TSC, 12 had ASD (29%). After controlling for age, TSC patients without ASD showed a small decrease in FA of the arcuate fasciculus compared to control subjects, and TSC patients with ASD had much lower FA than both control subjects and TSC patients without ASD. Similarly, while TSC patients without ASD had only a small increase in MD compared to control subjects in the arcuate fasciculus, TSC patients with ASD had much higher MD than control subjects and TSC patients without ASD.

A new method for assessing the microstructure of young patients showed similar results with decreased compactness in language pathways of TSC patients with ASD. Another new method designed to better analyze regions with crossing pathways showed modifications in language pathway microstructure that correlated with ASD diagnosis in the TSC patients. Preliminary analysis of neuropsychiatric data also showed a trend toward an association of arcuate fasciculus MD with verbal IQ, although the result was not significant after multiple comparisons correction.

It remains unclear why some patients with TSC develop ASD, while others have better language outcomes. Our results suggest that aberrant development of language pathways may act as a marker for poor neurological outcome in TSC patients. The impaired microstructure in language pathways of TSC patients may be responsible for the development of ASD, although prospective studies examining the development of language pathways and subsequent ASD diagnosis in this patient population remain essential. It is also possible that a primary problem with language leads to decreased use and subsequent poor development of language pathways. Early diagnosis of ASD is crucial for improving the outcomes of affected children.

Frequently-used abbreviations

AD = axial diffusivity; AF = arcuate fasciculus; ASD = autism spectrum disorders; FA = fractional anisotropy; IFOF = inferior fronto-occipital fasciculus; ILF = inferior longitudinal fasciculus; MD = mean diffusivity, RD = radial diffusivity; ROI = region-of-interest; SLF = superior longitudinal fasciculus; TSC = tuberous sclerosis complex; UF = uncinate fasciculus.

Summary

Tuberous sclerosis complex (TSC) is an autosomal-dominant neurocutaneous disease leading to disruption of the mTOR pathway. Inactivating mutations in *TSC1* (encoding hamartin) or *TSC2* (encoding tuberin) cause TSC. TSC has variable neurological outcomes, with many patients exhibiting little impairment, but between 17 and 61% showing signs of autism spectrum disorders (ASD), and approximately half with low IQ. Determining which patients are at risk for ASD may help guide treatment.

Diffusion tensor imaging (DTI) analysis of white matter microstructure in TSC and idiopathic ASD shows distinct abnormalities, particularly in language pathways for patients with ASD. This study aimed to examine TSC patients with and without ASD, as well as controls, to determine if changes in language pathways microstructure correlate with ASD diagnosis and verbal IQ.

I studied 42 TSC patients and 42 healthy controls who were scanned with diffusion-weighted MRI. I pre-processed the scans to remove motion artifacts and eddy current distortions and to align the diffusion data with the T1-weighted scan. To identify white matter pathways, I first manually selected regions-of-interest (ROIs) in template subjects. I then automatically mapped the ROIs to all patients and controls and used the ROIs to identify the superior longitudinal fasciculus (SLF), arcuate fasciculus (AF), inferior longitudinal fasciculus (ILF), uncinate fasciculus (UF), and inferior fronto-occipital fasciculus (IFOF).

12 of the 42 patients with TSC also had ASD (29%). Using traditional tractography statistical analysis, I found that TSC patients with ASD had increased AF mean diffusivity (MD) (suggesting diminished compactness) relative to both TSC patients without ASD and controls.

Similarly, TSC patients with ASD had decreased AF fractional anisotropy (FA) compared to both TSC patients without ASD and controls. I also found abnormalities in the SLF, ILF, and IFOF microstructure of TSC patients with ASD, although the UF microstructure appeared normal.

To further analyze the data for young patients, I developed a new method for studying language regions (rather than tracts) and used it to calculate AF microstructural parameters for all patients. After multiple comparisons correction, there were no significant predictors of verbal IQ (n = 11 patients with results from neuropsychiatric testing), but there was a trend toward an inverse correlation between AF MD and verbal IQ.

Finally, I developed a method for reducing the partial voluming effect in the calculation of tract volume and used it to determine the volume of each language tract. Both traditional tractography and my new method did not show any differences in patients compared to controls in tract volume, although my new method showed a trend toward differences in tract volume in patients with ASD that failed to reach significance after multiple comparisons correction.

This study is the first to examine language pathways in TSC and the second to correlate neuroimaging findings with ASD diagnosis. It is also the first to use a continuous language measure in TSC patients and correlate the language measure to AF microstructure. This study shows that language pathway microstructure correlates with neurological outcome in TSC patients. Eventually, DTI analyses of TSC patients may help guide treatment, allowing early therapy for those at risk of developing language deficits.

Future studies will look prospectively at TSC patients, determining if DTI markers of neurological risk correlate with prognosis. Correlating language pathway findings with later development of ASD or poor verbal IQ will help stratify risk in patients with TSC and inform treatment decisions.

1. Introduction

1.1 TSC background

Tuberous sclerosis complex (TSC) is an autosomal-dominant neurocutaneous disease caused by loss of either the *TSC1* (encoding hamartin) or *TSC2* (encoding tuberin) genes. *TSC1* and *TSC2* are tumor suppressor genes that respond to exogenous and endogenous signals to regulate cell size and growth. Together, they form a GTPase activating protein (GAP) complex with TSC1 stabilizing TSC2, and TSC2 containing the enzymatic GAP domain. Loss of either gene can lead to TSC, but patients with *TSC2* mutations have worse outcomes. Functionally, the TSC1/2 complex inhibits mTOR, which is involved in axon polarization and guidance as well as synapse formation and function. Rapamycin, a well-characterized inhibitor of mTOR, may be useful for patients with TSC, although its immunosuppressive effects necessitate identifying patients at risk for poor outcomes before attempting treatment (Han and Sahin 2011).

TSC is characterized by lesions throughout the body, most commonly affecting the brain, kidneys, skin, and lungs (Crino, Nathanson et al. 2006). TSC is a relatively common genetic syndrome with a birth incidence of 1 in 5800 (Osborne, Fryer et al. 1991). Among neurocutaneous disorders, TSC is second only to Neurofibromatosis Type 1 in prevalence (Baskin 2008). TSC is commonly diagnosed by dermatologists and more than 90% of TSC patients have skin lesions (Crino, Nathanson et al. 2006). See table I for a summary of TSC characteristics.

Between 55 and 75 percent of patients with TSC have renal angiomyolipomas, benign tumors composed of blood vessels, smooth muscle, and fat. Surgical removal of the tumors is typically avoided to spare kidney function. TSC patients do not have an increased lifetime risk of renal

carcinomas, but with a median age at diagnosis of 28, they develop the disease at a younger age than most renal carcinoma patients do (Crino, Nathanson et al. 2006).

The lungs are also often affected in TSC with 26-39% of women with TSC exhibiting radiologic signs of lymphangioleiomyomatosis (LAM) (Crino, Nathanson et al. 2006). LAM is often asymptomatic, at least initially, but patients with LAM may present with dyspnea or pneumothorax. Recent evidence suggests that LAM in TSC is caused by cells from renal angiomyolipomas that have seeded the lungs (Crino, Nathanson et al. 2006).

Infants with TSC exhibit cardiac rhabdomyomas, which can interfere with normal heart function in a small subset of these patients. Intramural or intracavitary tumors can interfere with conduction, leading to cardiac failure, complete heart block, and/or tachycardia in some infants. Unlike other hamartomas commonly seen in patients with TSC, cardiac rhabdomyomas usually regress without treatment, and typically affect only infants (Crino, Nathanson et al. 2006).

1.2 Neurologic symptoms

Neurologic symptoms are common in TSC and include epilepsy and socio-behavioral conditions like autism (Crino, Nathanson et al. 2006). Epilepsy is among the most common manifestations of TSC and cortical tubers may serve as foci for these seizures. Cortical tubers are found in 80% of TSC patients and their surgical resection is often required to treat drug-resistant epilepsy (Crino, Nathanson et al. 2006). Infantile spasms, a particularly severe form of epilepsy associated with cognitive deficits, occur in 20-30% of infants with TSC. The severity and duration of infantile spasms correlate with neurocognitive dysfunction, suggesting that seizures may be responsible for the deficits. Alternatively, a common mechanism may lead to both infantile spasms and neurocognitive difficulties (Crino, Nathanson et al. 2006).

1.2.1 ASD in TSC

ASD are common developmental disorders with a prevalence of 1 in 110 among children (2007). ASD remain difficult to diagnose in young children who do not have the language skills necessary for most testing. Between 17 and 61% of children with TSC exhibit symptoms of ASD (Asano, Chugani et al. 2001). The uncertainty in the exact proportion of TSC patients with ASD is due to the challenge of finding a representative population for TSC studies. Although cortical tubers seem to be related to epilepsy and may serve as foci for seizures, these tubers have a poorly defined relationship to neurocognitive deficits and to autism in particular (Walz, Byars et al. 2002) (Jansen, Vincken et al. 2008).

TSC patients with autism also have significantly more general cognitive impairment than patients without autism. Many TSC patients without autism have some cognitive impairment and have reduced scores on the autism diagnostic observation schedule (ADOS) (Jeste, Sahin et al. 2008). Early indicators of autism are extremely useful because early intervention can significantly improve the expected outcome for affected children. ASD in TSC correlates with early seizure activity and more frequent seizures (Numis, Major et al. 2011). It is unclear, though, if autism and frequent/early seizures have a common cause, or if the seizures themselves cause autistic symptoms directly.

1.2.2 General language delay in TSC

In addition to the association of TSC with ASD specifically, TSC patients also often have general language delay and cognitive deficits. Young TSC patients have a language delay of nearly five months at one year, and more than a year by three years of age (Humphrey, Higgins et al. 2004). Seizure activity may predict cognitive function and intelligence. Age at seizure

onset predicted cognitive score in one study (Jansen, Vincken et al. 2008) and infantile spasms have been linked to mental retardation (Goh, Kwiatkowski et al. 2005).

A study of intelligence quotient (IQ) and developmental quotient (DQ) in TSC patients found a bimodal distribution with the variability perhaps related to seizure activity. The upper curve showed a mean IQ/DQ 92.5, while the lower curve had a mean IQ/DQ of 44.6. None of the patients with a seizure onset after 2.5 years of age had an IQ/DQ below 70 (Winterkorn, Pulsifer et al. 2007).

1.3 DTI findings in TSC

TSC patients show abnormalities in brain microstructure with diffusion tensor imaging (DTI). Diffusion tensor imaging is one strategy for early detection and characterization of brain abnormalities and may be useful for autism diagnosis. See table II for a summary of DTI findings in TSC.

Microstructural characteristics of brain white matter are important indicators of development. Between 12 and 18 years of age, fractional anisotropy (FA) increases in the developing brain while mean diffusivity (MD) decreases. In most studies, higher FA and lower MD correlate with improved cognitive function. These correlations vary depending on the measures of cognitive ability, region of the brain studied, and population evaluated (Schmithorst and Yuan 2010). See table III for a brief summary of the microstructural measures commonly used in DTI studies.

The diffusion microstructure of tubers is significantly different from unaffected contralateral regions and corresponding areas in controls and perilesional white matter is also affected (Peng, Lee et al. 2004) (Karadag, Mentzel et al. 2005). Cortical tubers have an increased

apparent diffusion coefficient (ADC) and significantly decreased fractional anisotropy (FA) compared to contralateral normal-appearing white matter (NAWM) (Piao, Yu et al. 2009). The tubers also exhibit variability over time, growing and changing rather than remaining static (Chu-Shore, Major et al. 2009).

The relationship between tubers and important clinical findings—including epilepsy, autism, and mental retardation—remains poorly characterized. In one study, infantile spasms related to cortical tuber location (parietal and occipital lobes) and age related to the presence of tubers ($p = .047$), but there was no correlation between tuber presence or location and other clinical variables (Wong and Khong 2006).

Differences in gray matter or NAWM may better predict neurological symptoms in TSC. Patients with TSC have decreased subcortical gray matter and interhemispheric white matter (Ridler, Suckling et al. 2007). Within the NAWM, mean diffusivity is increased and fractional anisotropy decreased compared to controls. (Makki, Chugani et al. 2007). Changes in TSC patients relative to controls have consistently been found in the corpus callosum, geniculocalcarine tracts, and internal capsule (Krishnan, Commowick et al. 2010) (Simao, Raybaud et al. 2010), as well as more diffusely in long-range connections (Wong, Wang et al. 2013). The changes in NAWM may be age-dependent, with changes seen in one study only in children older than 8 years of age (Arulrajah, Ertan et al. 2009).

1.4 DTI findings in idiopathic ASD

DTI has also been used to identify brain structural changes in patients with idiopathic autism, particularly in language pathways. MD appears to be decreased throughout the brains of autistic patients (Groen, Buitelaar et al. 2011). Specific changes in the brains of patients with ASD

correlate with outcomes including social impairment and cognitive processing speed (Noriuchi, Kikuchi et al. 2010) (Alexander, Lee et al. 2007). A recent meta-analysis of DTI studies suggests that long-range association pathways in patients with ASD have reduced FA relative to typically-developing controls, particularly in the corpus callosum, left uncinate fasciculus, and left longitudinal fasciculus (Aoki, Abe et al. 2013).

Language tracts have been of particular interest to investigators studying the neuroanatomical correlates of autism. Autistic patients exhibit significant variability in language ability and women have better socio-communication skills (Lai, Lombardo et al. 2011). Language deficits may be among the first problems seen in toddlers who develop autism, with decreases in interhemispheric brain activity synchronization correlated to ASD status (Dinstein, Pierce et al. 2011).

1.4.1 The arcuate fasciculus: ASD, normal function, and other diseases

The arcuate fasciculus is the major fiber tract that connects the two classical centers of language: Wernicke's and Broca's Areas. Wernicke's Area is typically found in the superior temporal gyrus and is essential for receptive language. Broca's Area is found in the inferior frontal gyrus and classically supports language production. In normal patients, the left arcuate fasciculus is considerably better-developed than the right-sided tract (Geschwind and Levitsky 1968). For the purposes of this study, Wernicke's Area and Broca's Area are defined by anatomic criteria following a well-defined strategy developed by Catani, Jones, and colleagues (2005). In patients with ASD, AF laterality is less pronounced and FA is reduced (Upadhyay, Hallock et al. 2008) (Knaus, Silver et al. 2010; Jeong, Sundaram et al. 2011).

In normal subjects, the AF microstructure is also related to language function. The diffusivity of the left AF correlates with phonological awareness skills, while the volume lateralization of the

arcuate correlates with phonological memory and reading ability (Yeatman, Dougherty et al. 2011). Similarly, children with an AF identifiable only on the left side had significantly better vocabulary and phonological processing scores (Lebel and Beaulieu 2009). A separate study showed that AF left lateralization correlates with reading scores in first graders (Qiu, Tan et al. 2011).

Changes in the AF have also been identified in a variety of diseases. In patients recovering from strokes, the lesion burden in the arcuate fasciculus correlates with speech impairment. (Marchina, Zhu et al. 2011). In schizophrenics, the FA of the AF predicts the presence of auditory hallucinations (de Weijer, Neggers et al. 2011). Patients with temporal lobe epilepsy, Angelman Syndrome, and congential bilateral perisylvian syndrome also have changes in AF microstructure that correlate with language outcome (Kim, Chung et al. 2011) (Wilson, Sundaram et al. 2011) (Bernal, Rey et al. 2010; Saporta, Kumar et al. 2011).

1.4.2 Other language pathways in ASD

Several other putative language pathways show changes in ASD, although their role in language remains the subject of debate. See table IV for a summary of the putative language pathways studied in this thesis. Some fMRI evidence suggests the SLF and AF together comprise a dorsal stream for mapping sound to articulation, with a ventral extent of the ILF and IFOF assigning sound to meaning (Saur, Kreher et al. 2008). Stimulation of the IFOF induces semantic paraphasia and AF stimulation leads to phonological paraphasia. Surprisingly, stimulation and eventual resection of a portion of the ILF does not lead to language deficits (Mandonnet, Nouet et al. 2007). SLF stimulation leads to deficits in speech perception and articulation (Duffau, Peggy Gatignol et al. 2008). In contrast, stimulation and the eventual removal of a portion of the UF do not lead to obvious language deficits, suggesting that although the UF is a multi-hemisphere association pathway, it may not have a clear role in language in

the normal brain (Duffau, Gatignol et al. 2009). The locations of the AF and IFOF from DTI agree very well with locations identified through electrostimulation (Leclercq, Duffau et al. 2010).

Adolescent ASD patients have increased diffusivity in the right ILF (Ameis, Fan et al. 2011), while other ASD patients show changes in the IFOF and SLF, although the changes do not correlate with social responsiveness (Jou, Mateljevic et al. 2011). Cognitive and behavioral therapies with augmentative communication lead to improved UF integrity in ASD patients. Increased UF integrity also independently predicts better outcomes in this group (Pardini, Elia et al. 2011). A separate study showed that patients with Asperger's had a higher UF MD than matched controls, which may be related to the socio-emotional role of the UF, rather than to language function (Pugliese, Catani et al. 2009).

More generally, patients with ASD may process language information differently from healthy controls. Some work suggests that central linguistic processes are bypassed in autistic children in favor of peripheral white matter (e.g. visuospatial regions) (Sahyoun, Belliveau et al. 2010).

1.5 Neuroimaging methods

1.5.1 Traditional tractography approach

Traditional tractography with DTI is frequently used to delineate and analyze brain white matter fiber pathways. DTI can be used to identify CNS pathology in humans and validate animal models of neurological illness. Many studies have already shown the reproducibility and accuracy of using DTI to recapitulate known connections (Catani, Jones et al. 2005; Hsu, Van Hecke et al. 2010) (Catani and Thiebaut de Schotten 2008; Ciccarelli, Catani et al. 2008) (Mori, Crain et al. 1999). Traditional tractography with DTI is particularly valuable for this thesis,

because the findings can easily be compared to other studies on TSC and ASD. See table V for a comparison of the methods used in this thesis.

Water diffusion in brain white matter can be described by microstructural variables indicating the speed of the diffusion (axial diffusivity, mean diffusivity, and radial diffusivity) and the directionality of the movement (fractional anisotropy). Microstructural characteristics of the brain extracted from DTI data describe changes in the brain due to development, traumatic injury, and disease processes. Song and colleagues showed that the *shiverer* mouse, known to exhibit dysmyelinated axons, had significantly higher RD, although the AD stayed the same (Song, Sun et al. 2002).

In 2003, the same group showed that decreased AD likely represents axon damage, while increased RD coincides with myelin degeneration. Axonal changes in a mouse model of renal ischemia lead to decreased AD without affecting RD. Subsequent myelin degeneration at five days after ischemia was accompanied by an increase in RD, but no further change in AD (Song, Sun et al. 2003). These results suggest that microstructural variables may be useful for tracking myelin and axonal deterioration. Microstructural variables may also be useful for analyzing the initial deposition of myelin and targeting of axons as well, although further study is needed.

Studies on schizophrenic patients show decreased FA in the prefrontal cortex of patients compared to normal controls, as well as decreased FA in long-distance fiber connections in young patients (Buchsbaum, Tang et al. 1998) (Jones, Catani et al. 2006). Microstructural data have also provided important insight into what portions of the brain develop first. Lebel and colleagues used DTI to show that areas with fronto-temporal connectivity develop more slowly (Lebel, Walker et al. 2008).

Studies of very young patients have shown that maturation likely occurs in the corticospinal and spinothalamic tracts and fornix, followed by language regions including the arcuate and inferior longitudinal fasciculi. The optic radiations were followed by the internal capsule and cingulum as the final tracts to mature (Dubois, Dehaene-Lambertz et al. 2008). Fractional anisotropy increases through childhood then slowly decreases thereafter (Hasan, Iftikhar et al. 2009). For adults, the anterior corpus callosum, anterior and posterior internal capsule on both sides, and the posterior periventricular regions show the largest age-related FA decreases. The temporal and occipital regions may not have age-related reductions in FA (Hsu, Leemans et al. 2008).

1.5.2 Template tract ROI approach

Despite the many successes of traditional tractography to determine the size and structural integrity of regions of the brain, it has some significant limitations. First, with current one-tensor modeling of DTI data, many complex tracts are difficult to segment or entirely absent in very young subjects. The AF is often difficult to find with traditional tractography in young patients because the brain has not adequately myelinated in this region (Thiebaut de Schotten, Ffytche et al. 2011).

In contrast, a ROI approach to studying language regions circumvents some of these drawbacks, while introducing others. For this study, I implemented a ROI approach by performing tractography in the set of template subjects, then mapping to patients and control subjects. In this way, I examined the expected regions for language development, even if traditional tractography did not identify such regions in individual patients or control subjects.

The ROI approach has the clear drawback of selecting regions that may not be anatomically connected in the patients. That is, although the shape of the regions is similar to the corresponding regions in the templates, the overall connections may be rather different. For this

reason, the ROI approach is less likely to reflect functional connections and instead gives information about general language region integrity. As noted, especially for complicated tracts, the ROI method may be superior to traditional tractography for assessing young patients.

1.5.3 Fractional occupancy approach

In addition to the challenge of finding the appropriate tracts in young patients with traditional tractography approaches, the method for calculating tract microstructural values remains rather primitive, subject to large deviations due to partial voluming effects (PVEs). In this thesis, I propose a new method that seeks to improve volume and microstructural variable calculation by reducing PVEs.

PVEs impair the calculation of FA, particularly when large voxels are used (Pfefferbaum, Adalsteinsson et al. 2003). Partial-voluming in tractography statistical analysis is a particular problem in brain tissue bordering free water including edema or cerebrospinal fluid (CSF). Voxels partially filled with free water have much lower fractional anisotropy values and higher mean diffusivity than tracts of white matter alone (Pasternak, Sochen et al. 2009).

Regions with crossing fibers have significantly higher FA values when small voxels are used, suggesting that PVEs inappropriately lower the calculated FA in areas with many crossing fibers (Oouchi, Yamada et al. 2007). Thus, partial voluming may lead to inaccurate measurements of diffusion tensors in areas with crossing fibers or adjacent free water (Bastin, Munoz Maniega et al. 2010). A two-tensor model with two compartments representing each voxel may better compensate for partial-voluming effects (Alexander, Hasan et al. 2001).

Current approaches count any voxel touched by the streamlines as fully contained within the fiber bundle of interest, even if several other fiber bundles pass through the same voxel and

contribute to diffusion of water in that region. Vos and colleagues recently showed that changing the bundle shape artificially changes bundle volumes and microstructural parameters when the PVE is not considered (Vos, Jones et al. 2011).

As an initial attempt to minimize PVEs, I performed additional analyses with a modified streamline strategy. I used a whole-brain streamline generation strategy, followed by segmentation and a novel voxel-wise volume and microstructure analysis. First, I generated streamlines by seeding from all regions of the white matter with high FA. Next, I created a segmentation of the brain, categorizing voxels as gray matter, CSF, or white matter. Using the white-matter segmentation, I excluded voxels that fell in gray matter or CSF. After selecting the tracts, I performed a voxel-wise analysis of the volume and statistics.

Even with the fractional occupancy method, it remains challenging to properly account for voxels that are partly occupied by CSF and/or gray matter in addition to white matter. Ideally, we would recognize these voxels and attempt to compensate for the proportion of the voxel occupied by each substance when making volume and microstructural variable calculations. Improvements in resolution will also make such PVEs less common and less likely to influence the findings.

1.6 Purpose of the study

Thus, while several groups have identified white matter abnormalities in patients with TSC and arcuate fasciculus microstructure helps predict neurological outcome in several diseases, nobody has examined the arcuate fasciculus in this group. Building from the studies connecting arcuate fasiciculus white matter integrity in a variety of pathologies, we examined a group of TSC patients and age-matched controls. The TSC patients have variable autism status. This

study aims to analyze the specific neurological deficits associated with ASD in this subgroup of patients with ASD. We investigated the microstructure of language tracts in the brain, including the well-characterized arcuate fasciculus (AF), as well as probable language tracts including the superior longitudinal fasciculus (SLF), inferior fronto-occipital fasciculus (IFOF), inferior longitudinal fasciculus (ILF), and the uncinate fasciculus (UF), a multi-hemisphere association pathway that does not appear to have a role in language. Linking deficits in language pathways to autism status may allow prediction of autism diagnosis in TSC patients from microstructural variables, leading to earlier treatment and improved outcomes.

2. Materials and Methods

2.1 Subjects

Subjects were recruited and imaged before I became involved in this study. I accessed all of the imaging data courtesy of a medical records IRB through Children's Hospital Boston (CHB). The study involved 42 patients (ages 1 – 25 years) diagnosed with TSC and 42 age-matched control subjects. All were imaged with 3T magnetic resonance imaging (Siemens Trio from Siemens, in Munich, Germany). Data from six of the age-matched controls were obtained with the same acquisition protocol from collaborators at the University of North Carolina (Chapel Hill). Dr. Sanjay Prabhu, a pediatric neuroradiologist, reviewed each MRI, and all control subjects had a normal MRI.

Dr. Mustafa Sahin diagnosed all 42 patients with TSC, as defined by the Tuberous Sclerosis Consensus Conference (Roach, DiMario et al. 1999).

All TSC patients were followed in the Multidisciplinary Tuberous Sclerosis Program at CHB. The ASD diagnoses were based on clinical assessment by a board certified pediatric neurologist (Dr. Mustafa Sahin and/or Dr. Shafali Jeste). In all but the three oldest subjects, the Diagnostic and Statistical Manual DSM-IV-TR (American Psychiatric Association, 2000) was supplemented by the Autism Diagnostic Observation Schedule (ADOS) by experienced specialists (Vanessa Vogel-Farley or Dr. Shafali Jeste). Recruitment of subjects and data acquisition were conducted with informed consent, using a protocol approved by the IRB of Children's Hospital Boston.

2.2 Data acquisition and analysis

The MRI protocol included routine clinical imaging and a diffusion imaging addition. Sedation was used for clinical imaging when necessary to prevent significant motion. The imaging protocol included a T1w MPRAGE and a T2w TSE, with diffusion imaging (Reese, Heid et al. 2003) acquired in the axial plane. The diffusion imaging comprised 30 slices with b=1000 s/mm^2 and 5 b=0 images. The diffusion imaging protocol was designed by Dr. Simon Warfield

I used imaging tools developed in the Computational Radiology Laboratory (CRL; director Dr. Simon Warfield) to segment the intracranial cavity following the structural MRI (Grau, Mewes et al. 2004) (Weisenfeld and Warfield 2009). The diffusion images were aligned to the T1w magnetization-prepared rapid gradient-echo (MPRAGE) image to compensate for distortion and patient motion (Ruiz-Alzola, Westin et al. 2002). The tensor fit was estimated with robust least-squares (Douek, Turner et al. 1991). The resolution of the T1w MPRAGE (and thus the final resampled (interpolated) resolution) varied somewhat among the subjects, although most were resampled to 1mm x 0.78 mm x 0.78 mm. See Figure 1 for a schematic showing the steps in pre-processing the raw DTI data.

2.3 Tractography

For tractography, I used a stochastic algorithm developed in the Warfield lab that combines the speed and accuracy of deterministic decision-making at each voxel with probabilistic sampling to better explore the space of all possible streamlines. In particular, the algorithm combines deterministic sub-voxel steps with small stochastic modifications to allow the exploration of alternate routes. The stochastic modifications also allow the tracking of multiple streamlines from a single voxel. Because the voxels (1 mm x 0.78 mm x 0.78 mm) may contain several crossing or diverging fiber tracts, allowing for multiple streamlines within a single voxel is essential for accurate assessment of fiber connectivity.

To initiate streamlines in an unbiased manner, I used a seeding region including all brain white matter with high fractional anisotropy (above 0.4). Streamlines were constructed with sequential steps through the tensor field at sub-voxel resolution (Lazar, Weinstein et al. 2003). While evaluating each streamline, I programmed the algorithm to check conventional stopping criteria, including streamline curvature and weighted fractional anisotropy, with a maximum curvature angle of 45 degrees, and a minimum weighted fractional anisotropy of 0.15.

Again using the tractography algorithm developed in the Warfield lab, I incorporated the prior path of the streamline to compensate for local inhomogeneities by assigning a momentum to the direction and fractional anisotropy calculations. For assessing endpoint criteria, the streamline FA and direction at a given voxel is a weighted average of the values for all the recent voxels, with more recent voxels attaining a higher weight. Thus, if we define tensor deflection fraction τ as a constant between 0 and 1, we can express the direction for the nth step recursively as (where d_n is the direction at the nth voxel, γ is the tensor deflection fraction, δ is the current tensor proportion, ε is the tensor deflection power):

$$\overrightarrow{d_n} \propto \tau * \left(\overrightarrow{d_{n-1}}\right) + (1-\gamma) * [\delta * \overrightarrow{D_n}^{\varepsilon} * \overrightarrow{d_{n-1}} + (1-\delta) * (\overrightarrow{v_n})] \mid \overrightarrow{d_1} = \overrightarrow{v_1}$$

For this project, I defined τ = 0.9, δ = 0.5, ε = 2.

Similarly, if we define a fraction u as a constant between 0 and 1 as the fractional anisotropy momentum, we can define the weighted fractional anisotropy of the nth step (used only for stopping criteria, not statistics) recursively:

$$w_n = u * a_n + (1-u) * w_{n-1} \mid w_1 = a_1$$

For this project, I defined fractional anisotropy momentum u = 0.5. As stated above, I set the FA minimum to be 0.15.

Finally, to check for the curvature of a streamline, the angle change θ is computed for each step (where β is the angular momentum, $v_{n_j}$the jth component of the nth eigenvector, and d_{n-1_j} is the jth component of the n-1st direction.

$$\theta_n = \beta * \theta_{n-1} + (1-\beta) * \sum_{j=1}^{3} v_{n_j} d_{n-1_j}$$

To determine the total angle, the cosines of successive angles are summed and the overall angle assessed by taking the inverse of cosine of the sum. As stated above, I set the angle maximum to 45 degrees.

Streamlines were estimated with log-Euclidean tensor interpolation (Arsigny, Fillard et al. 2006) at each voxel. The range of potential streamlines examined is broad compared to conventional deterministic tractography. Stochastic sampling was continued until a predetermined number of streamlines had been created for the whole brain.

2.4 Selection

Furthermore, as proposed by Wakana and colleagues (Wakana, Jiang et al. 2004), I specified regions-of-interest (ROIs) to ensure streamlines followed the known anatomy. I modified the classical approach slightly by defining required endpoint regions for the streamlines based on prior methods used to identify the arcuate fasciculus (Catani, Jones et al. 2005). I used the endpoint regions only for the selection of the streamlines, not for streamline generation. I selected streamlines that ended near certain regions-of-interest (selection ROIs), and excluded those that did pass through other regions-of-interest (exclusion ROIs) to identify the tracts of interest bilaterally, including the arcuate fasciculus (AF), superior longitudinal fasciculus (SLF), inferior fronto-occipital fasciculus (IFOF), inferior longitudinal fasciculus (ILF), and uncinate fasciculus (UF).

2.5 ROI generation

To generate ROIs automatically for a large number of subjects, I delineated each ROI in a set of twenty template brains. Using the Simultaneous Truth and Performance Level Estimation (STAPLE) algorithm (Warfield, Zou et al. 2004) modified by Dr. Ralph Suarez in the CRL to work with a set of selection or exclusion ROIs (Suarez, Commowick et al. 2011), I mapped each ROI from the template brains onto each TSC patient and control subject, and selected the consensus voxels. For the template brains, the AF and SLF ROIs were delineated by inspection

of the color-coded tensor image, and tracts were selected using a two ROI approach (Catani, Jones et al. 2005).

For the arcuate fasciculus, I specified ROIs in the white matter near Broca's Area and Wernicke's Area and required streamlines constituting the tract to pass through both. For the superior longitudinal fasciculus, I specified ROIs in the white matter near Broca's Area and in the parietal lobe near Geschwind's territory, following the method defined in tractography work by other authors (Catani, Jones et al. 2005).

Similarly, the IFOF, ILF, and UF were selected with a two ROI approach based on a previously published atlas (Catani and Thiebaut de Schotten 2008). For the IFOF, I specified ROIs in the occipital and frontal lobes and selected streamlines that touched both. For the ILF, I specified ROIs in the occipital and temporal lobes, while for the UF I specified ROIs in the temporal and frontal lobes. Figures 4, 5, and 6 show the ROIs and selected streamlines for a TSC patient with ASD, a TSC patient without ASD, and a control subject (respectively; 'selection ROIs' and 'selected streamlines (with T1 image)'). For statistical analyses, the fractional anisotropy (FA), mean diffusivity (MD), axial diffusivity (AD) and radial diffusivity (RD) were derived from each tensor.

Mathematically, MD is defined as the mean of the eigenvalues for the tensors at a given voxel:

$$MD = \frac{\lambda_1 + \lambda_2 + \lambda_3}{3}$$

FA is the normalized standard deviation of the three eigenvectors and is defined as:

$$FA = \sqrt{\frac{3}{2}} \sqrt{\frac{(\lambda_1 - \hat{\lambda})(\lambda_2 - \hat{\lambda})(\lambda_3 - \hat{\lambda})}{\lambda_1^2 + \lambda_2^2 + \lambda_3^2}} \mid \hat{\lambda} = MD = \frac{\lambda_1 + \lambda_2 + \lambda_3}{3}$$

Importantly, the FA is unitless and varies between 0 (perfectly isotropic, i.e. $\lambda_1 = \lambda_2 = \lambda_3$) and 1 (perfectly anisotropic, i.e. $\lambda_1 > 0; \lambda_2 = \lambda_3 = 0$.

RD is defined as the mean of the two minor eigenvalues:

$$RD = \frac{\lambda_2 + \lambda_3}{2}$$

AD is simply the principal eigenvalue:

$$AD = \lambda_1$$

All diffusivities (MD, RD, AD) have units of m^2 / s.

2.6 Tract ROI generation

The streamlines created by stochastic tractography and selected with white matter ROIs were then used to delineate a ROI for the assessment of white matter microstructural integrity. Voxels touched by fewer than three percent of the streamlines in the tract of interest were excluded from the analysis.

For the traditional tractography method, average parameters (FA, MD, AD, and RD) were assessed by computing the mean of each parameter over all voxels in the ROI (Powell, Parker et al. 2006) (Kubicki, Alvarado et al. 2011). Similarly, the volume of each tract was determined

by summing the volume of all voxels touched by more than three percent of the streamlines within a tract of interest. See figure 2 for a schematic showing the order of analysis for each of the methods used in this thesis.

2.7 Template tract ROI approach

For the template tract ROI approach, I generated streamlines in each of the template subjects following the previously described approach (see tractography, above). Next, I selected tracts in each template subject using the hand-drawn ROIs for each template subject. Using the selected streamlines, I generated tract ROIs in each of the template subjects and for each tract (AF, SLF, IFOF, ILF, UF; see tract ROI generation, above).

I mapped these tract ROIs onto each control subject and TSC patient with the STAPLE algorithm and the new mapping method developed in the Warfield lab (Suarez, Commowick et al. 2011). Each tract ROI from the normal templates was used to define the corresponding region in control subjects and TSC patients, marking the expected regions for the development of each language tract. Figures 4, 5, and 6 show the template tract ROIs that were mapped to a TSC patient with ASD, a TSC patient without ASD, and a controls subject (respectively; 'template tract ROI method'). I used these tract ROIs directly to assess microstructural variables (FA, MD, AD, RD) over all the voxels touched by these tract ROIs (see Tract ROI Generation, above, for the calculation of statistics from tract ROIs).

I also examined the FA laterality for each of the pathways. The simple FA laterality was calculated using the following formula, which ranges from -1 (complete right lateralization) to 1 (complete left lateralization):

FA laterality = $(FA_{left} - FA_{right}) / (FA_{left} + FA_{right})$

2.8 Fractional occupancy approach

For the fractional occupancy approach, I used the same streamline generation and selection methods as for the traditional tractography approach. To analyze the data, however, I used a novel method for calculating tract-based spatial statistics. First, I used a white matter segmentation to remove all portions of the tract that leave the white matter – this study aims to find volumes in white matter alone. The segmentation was developed in the lab by Dr. Alireza Akhondi-Asl and uses manually-segmented template subjects and the STAPLE algorithm to separate white matter from gray matter. As with the traditional tractography approach, I selected streamlines comprising each tract of interest from the set of all streamlines for the whole brain based on anatomical criteria.

For each tract of interest, I then calculated the fractional occupancy of the tract at each voxel. For example, suppose I am analyzing the arcuate fasciculus. For each voxel touched by the arcuate fasciculus, I divided the number of streamlines within the arcuate fasciculus by the total number of streamlines for the whole brain that pass through that voxel. Figure 3 shows a two-dimensional representation of a voxel touched by both the arcuate fasciclus and the superior longitudinal fasciculus. Next, we multiply this fractional occupancy by the total volume of the voxel, and sum over all voxels touched by the arcuate fasciculus. This sum gives us the volume of our tract of interest (the arcuate fasciculus, in this case). For the following equation, $s_{i_{AF}}$ = # of arcuate fasciculus streamlines in the ith voxel. Similarly, $s_{i_{total}}$ = total # of streamlines in the ith voxel. v_i = volume of the ith voxel. The sum is over all voxels in the brain (arbitrarily ordered from 1 to n).

$$volume\ of\ the\ AF = \sum_{i=1}^{n} \frac{s_{i_{AF}}}{s_{i_{total}}} v_i$$

Similarly, I calculated microstructural statistics with weights based on the fractional occupancy of the tract in each voxel (normalizing by the sum of the streamline fractions alone over all the voxels). Thus, for the FA, I calculated the mean with fractional occupancy weights in each voxel. For the following equation, $s_{i_{AF}}$ = # of arcuate fasciculus streamlines in the ith voxel. Similarly, $s_{i_{total}}$ = total # of streamlines in the ith voxel. a_i = FA of the ith voxel. The sum is over all voxels (arbitrarily ordered from 1 to n).

$$mean\ FA = \frac{\sum_{i=1}^{n} \frac{s_{i_{AF}}}{s_{i_{total}}} a_i}{\sum_{i=1}^{n} \frac{s_{i_{AF}}}{s_{i_{total}}}}$$

The mean MD was calculated with MD weights in each voxel based on the streamline fraction. For the following equation, $s_{i_{AF}}$ = # of arcuate fasciculus streamlines in the ith voxel. Similarly, $s_{i_{total}}$ = total # of streamlines in the ith voxel. d_i = MD of the ith voxel. The sum is over all voxels (arbitrarily ordered from 1 to n).

$$mean\ MD = \frac{\sum_{i=1}^{n} \frac{s_{i_{AF}}}{s_{i_{total}}} d_i}{\sum_{i=1}^{n} \frac{s_{i_{AF}}}{s_{i_{total}}}}$$

2.9 Neuropsychiatric data

Data for the neuropsychiatric comparisons were collected by Dr. Rachel Hundley at the CHB Developmental Medicine Center. Dr. Hundley used different tests for each patient based on her professional judgment. For the preliminary neuropsychiatric analyses presented here, I selected only those patients who had data from normalized IQ testing with verbal IQ scores. Each measure has a mean of 100 and a standard deviation of 15. Because of the *ad hoc* collection

for clinical diagnosis, I used a variety of IQ tests. For one patient, I used Stanford-Binet (S-B) scores, for three others Bayley Scales of Infant and Toddler Development (third edition) (Bayley III), for one the Vineland Adaptive Behavior Scales (second edition) (VABS II), for three the Wechsler Preschool and Primary Scale of Intelligence (third edition) (WPPSI III), for one the Differential Ability Scales (DAS), and for two the Wechsler Intelligence Scale for Children (fourth edition) (WISC IV).

For verbal IQ measure, I chose the verbal IQ from the S-B test, language IQ from the Bayley III, communication score from the VABS II, the arithmetic mean of the verbal and language scores from the WPPSI III, the verbal IQ score from the DAS, and the verbal comprehension IQ score from the WISC IV.

For the non-verbal IQ measure, I chose the nonverbal IQ from the S-B test, the arithmetic mean of the nonverbal and motor IQ scores for the Bayley III, the arithmetic mean of the behavior composite, daily living, socialization, and motor skills IQ from the VABS II, the performance IQ from the WPPSI III, the non-verbal IQ score from the DAS, and the arithmetic mean of the perceptual reasoning, working memory, and processing speed scores from the WISC IV.

I calculated the performance to verbal IQ split by taking the nonverbal IQ score and subtracting the verbal IQ.

2.10 Statistical analysis

The DTI microstructural measures and volume were considered response variables in a regression model with age, sex, and group status. In separate analyses, I used the microstructural variables calculated with the traditional tractography, template tract ROI, and

fractional occupancy methods; I used the volume calculated with the traditional tractography and fractional occupancy methods. I split the subjects into three groups based on both TSC and ASD diagnoses. The groups included control subjects, TSC patients without ASD, and TSC patients with ASD. By examining scatterplots of the data, I determined that the age variable required log-transformation. In building the regression model, I considered all two-way interactions. I included only variables that improved the adjusted r^2 value of the model. In most cases, only group and the natural logarithm of age (log(age)) were identified as important terms. Sex was typically not significant once log(age) and group status were included in the models. I considered P-values of < 0.05 to be statistically-significant within each multiple linear regression model. I fit a distinct model for each microstructural variable/volume and each tract (AF, SLF, IFOF, ILF, UF).

For multiple comparisons correction, I used Bonferroni correction to define the p-value required for statistical significance in the study as a whole. I set the number of comparisons for Bonferroni correction to the number of multiple linear regressions performed for a given method. Thus, for the traditional tractography method, I set the number of comparisons as 15 (volume, FA, and MD for the five pathways studied), with p-value for significance set at $0.05/15 = 0.003$. For the template tract ROI method, laterality was included as a variable, in addition to FA and MD, so I set the p-value for significance at $0.05/15 = 0.003$. For the fractional occupancy method, volume was included as a variable for each tract, in addition to FA and MD, so I set the p-value for significance at $0.05/15 = 0.003$.

For the group of patients with neuropsychiatric data, I created additional regression models with the verbal IQ or performance to verbal IQ split as response variables with age, sex, group status, and microstructural variables (FA and MD for the SLF, AF, IFOF, ILF, and UF) as predictors. I used the microstructural variables calculated with the ROI method. As before, I split

the subjects into three groups based on TSC status and ASD diagnosis. I considered all two-way interactions while generating the models. For multiple comparisons correction, I used the number of multiple linear regressions. Thus, predictors were considered significant in the overall experiment for p-values less than 0.05/14 = 0.004.

3. Results

3.1 Patients

42 subjects (28 boys, 14 girls; mean age, 9.9 years; age range 1 – 27 years, median age 8.6 years) underwent diffusion-weighted MR imaging. The study also included 42 age-matched controls (20 boys, 22 girls; mean age, 9.9 years; age range 1 – 25 years, median age 8.7 years) with clinically-normal MRIs.

Unless otherwise specified, the results refer to the left-sided (typically the dominant side for language) tracts. For each tract and measure, a regression model was created as discussed in the methods; p-values are uncorrected and reflect the significance of predictors in the regression model. For the traditional tractography and fractional occupancy approaches, some subjects did not have any selected streamlines within a given tract. These data were treated as missing (not zero) for the regression analyses.

For each tract, I compared the groups while controlling for LOG(Age) (included as a predictor in every regression). I also examined the influence of sex, although it was only a significant predictor for one comparison. In general, FA increases with age, and is decreased in TSC patients. For some tracts, I saw a further decrease in FA in TSC patients with ASD. MD typically

decreases with age, and is increased in TSC patients. For many of the tracts studied, I found a further increase in MD in TSC patients with ASD.

3.2 Traditional tractography

As noted, after Bonferroni correction, the p-value for significance was set at 0.003. There were no group differences in volume for any of the tracts studied. The regression models for all tracts from the traditional tractography method are shown in table VI. The scatterplots of FA and MD vs. age for the traditional tractography method are shown in figures S1 and S2 (respectively).

3.2.1 SLF

Patients with ASD had a decreased FA relative to controls ($p = 8.21E-04$), but not patients without ASD ($p = 0.048$). Patients without ASD did not show a difference in FA relative to controls ($p = 0.060$). Patients with ASD had MD values that decreased more slowly with age than controls ($p = 4.69E-06$), but not compared to patients without ASD ($p = 0.011$). Patients without ASD had MD values that decreased similarly with age compared to their control counterparts ($p = 0.005$), although there was a trend toward a larger decrease with age that was not statistically significant after multiple comparisons correction.

3.2.2 AF

Patients with ASD had a decreased FA relative to both controls ($p = 7.44E-06$) and patients without ASD ($p = 0.003$). Patients without ASD had similar FA to controls ($p = 0.041$). Patients with ASD had a lower MD compared to both controls ($p = 5.41E-08$) and patients without ASD ($p = 5.48E-05$), and the difference was highly statistically-significant. Patients without ASD had similar MD to controls ($p = 0.038$).

After finding a difference in MD in these groups, I also looked at AD and RD to determine if the differences in MD were driven primarily by changes in either parallel (AD) or perpendicular (RD) diffusion. Patients with ASD had an increased AD relative to both controls (p = 8.98E-06) and patients without ASD (p = 0.002). Patients without ASD did not have a different AD than controls (p = 0.073). Similarly, patients with ASD had a higher RD than controls (p = 9.88E-08) and patients without ASD (p = 6.29E-05), but patients without ASD did not have a different RD than controls (p = 0.054).

3.2.3 ILF

Patients with ASD had a higher initial FA than controls (p = 0.003), but not patients without ASD (p = 0.010), and the FA for patients with ASD decreased more quickly with age compared to both controls (p = 7.92E-05) and patients without ASD (p = 6.53E-04). Patients with ASD had a similar initial MD to controls (p = 0.037) and to patients without ASD (p = 0.117). The MD of patients with ASD actually increased with age, different from both controls (p = 1.65E-04) and patients without ASD (p = 0.003) who had decreasing MD with age.

3.2.4 UF

For FA, there were no significant predictors across all three groups, with sex failing to reach the cut-off for statistical significance after correction for multiple comparisons (p = 0.015). After controlling for age, no other predictors improved the model for predicting UF MD.

3.2.5 IFOF

Patients with ASD had a similar starting FA to controls (p = 0.011) and patients without ASD (p = 0.070). The FA for patients with ASD actually decreased with age, however, significantly different from controls (p = 5.09E-04), but not patients without ASD (p = 0.011).

Patients with ASD had a similar starting MD to both controls (p = 0.035) and patients without ASD (p = 0.023). Patients with ASD also had a similar change in MD with age compared to both controls (p = 0.006) and patients without ASD (p = 0.003), although the change in MD narrowly missed the cut-off for statistical significance after correction for multiple comparisons.

After finding differences in TSC patients with ASD, I decided to examine whether right-sided pathways followed the same general trends as left-sided tracts. I examined the right SLF MD and right ILF MD. There were not enough data to examine the right AF.

3.2.6 Right SLF

MD for patients with ASD decreased more slowly with age than controls (p = 4.90E-04), but the rate of decrease with age was similar to patients without ASD (p = 0.041). There was no difference in MD between patients without ASD and controls (p = 0.057).

3.2.7 Right ILF

MD for patients with ASD decreased more slowly with age than controls (p = 9.94E-07), although the change with age did not differ compared to patients without ASD (p = 0.327). Patients without ASD had a similar initial MD compared to controls (p = 0.018).

Finally, after finding significant differences in multi-hemisphere association pathways in the group as a whole, I examined the data for patients younger than 10 years of age specifically to see if changes were evident in younger patients.

3.2.8 Patients younger than 10, AF

Young patients with ASD had a similar FA to young controls (p = 0.018) as well as young patients without ASD (p = 0.224). Young patients without ASD did not have a different FA than

young controls (p = 0.118). Young patients with ASD had a similar MD to controls (p = 0.007) and young patients without ASD (p = 0.138). Young patients without ASD did not have a different MD than young controls subjects (p = 0.121).

3.3 Template tract ROI

As noted, the p-value for statistical significance was set to 0.003 after Bonferroni correction for multiple comparisons. The regression models for all tracts from the template tract ROI method are shown in Table VII. The scatterplots of FA laterality, FA, and MD vs. age for the template tract ROI method are shown in Figures S3, S4, and S5 (respectively).

3.3.1 SLF:

The FA for patients with ASD decreased more rapidly with age than the FA for both controls (p = 1.19E-04) and patients without ASD (p = 0.001). Patients without ASD had a similar initial FA to controls (p = 0.009). MD for patients with ASD decreased with age at a similar rate to MD in controls (p = 0.027). The MD for patients without ASD decreased with age at a similar rate to the MD for controls (p = 0.034).

3.3.2 AF:

The FA for patients with ASD decreased more rapidly with age than the FA for both controls (p = 1.16E-06) and patients without ASD (p = 4.15E-04). Patients without ASD had a similar initial FA to controls (p = 0.016). Patients with ASD had a similar initial MD to both controls (p = 0.029) and patients without ASD (p = 0.009), but actually had an increasing MD with age, different from both controls (p = 9.33E-05) and patients without ASD (p = 3.28E-04). Patients without ASD had a higher MD than controls (p = 0.003).

3.3.3 ILF:

Patients with ASD had a rightward shift in ILF laterality compared to controls (p = 0.002), but the laterality was similar to patients without ASD (p = 0.006). Patients with ASD also had a smaller increase in FA with age than controls (p = 1.76E-08) and patients without ASD (p = 6.41 E-07). Patients with ASD had similar initial MD compared to both controls (p = 0.008) and patients without ASD (p = 0.005), but an increasing MD with LOG(Age), different from both controls (p = 4.25E-05) and patients (p = 2.20E-04). Patients without ASD had a similar MD to controls (p = 0.011).

3.3.4 UF:

Patients with ASD had a similar increase in FA with age to controls (p = 0.006) and patients without ASD (p = 0.020). For MD, there were no differences based on group status.

3.3.5 IFOF:

Patients with ASD had a rightward shift in IFOF laterality compared to controls (p = 0.001). Patients with ASD had a smaller increase in FA with age than controls (p = 3.00E-07) and patients without ASD (p = 2.61E-05). Similarly, patients with ASD had a smaller decrease in MD than controls (p = 1.16E-05) and patients without ASD (p = 3.79E-04).

3.3.6 Right AF:

Further analysis was performed on the right AF after it was determined that there was a difference in microstructure of the left AF in patients with ASD compared to controls and patients without ASD. Patients with ASD had a slower decrease in MD than controls (p = 4.27E-09) and patients without ASD (p = 0.003). Patients without ASD also had a higher initial MD than controls (p = 2.21E-04).

3.4 Fractional Occupancy

The regression models for all tracts from the fractional occupancy method are shown in Table VIII. The scatterplots of tract volume, FA, and MD vs. age for the fractional occupancy method are shown in Figures S6, S7, and S8 (respectively). As noted in the methods, the p-value for statistical significance was set at 0.003 after Bonferroni correction.

3.4.1 SLF:

Patients with ASD had a similar increase in FA compared to both controls (p = 0.027) and patients without ASD (p = 0.099). Patients with ASD also had a slower decrease with age in MD than controls (p = 2.27E-05), but a similar decrease with age to patients without ASD (p = 0.025). Patients without ASD had a similar initial MD compared to controls (0.008).

3.4.2 AF:

The volume of the AF was similar in patients without ASD compared to controls (p = 0.044). Patients with ASD had a lower FA than controls (p = 5.33E-06), but a similar FA to patients without ASD (p = 0.012). Patients without ASD had a similar FA to controls (p = 0.005). For the MD, patients with ASD had a slower decrease than controls (p = 3.19E-08), but no difference from patients without ASD (p = 0.098).

3.4.3 ILF:

The initial FA was similar in patients with ASD and controls (p = 0.020), as well as patients without ASD (p = 0.017). The FA actually decreased with age for patients with ASD, though, in contrast to the increase in controls (p = 9.16E-04) and patients without ASD (p = 0.001). Similarly, the MD actually increased with age for patients with ASD, while decreasing in controls

(p = 0.002). For patients with ASD, there was no difference in the change in MD with age compared to patients without ASD (p = 0.036).

3.4.4 UF:

Males had no difference in FA compared to females (p = 0.010). There were also no differences in FA by group status (controls, TSC patients without ASD, or TSC patients with ASD). Only LOG(Age) was a significant predictor of UF MD.

3.4.5 IFOF:

Patients with ASD had a similar increase in volume compared to controls (p = 0.008) and patients without ASD (p = 0.019). FA did not vary by group status, although it did increase with age. Similarly, the only significant predictor of MD was LOG(Age).

3.5 Neuropsychiatric data

The regression models for all tracts from neuropsychiatric analyses are shown in Table IX. As noted, for the overall analysis, a p-value of 0.004 was used after Bonferroni correction.

11 patients had sufficient data to attempt prediction of the language/verbal IQ as well as prediction of the non-verbal to verbal IQ split. There were 7 males and 4 females in the neuropsychiatric group, with an age range of 2-10. Four of the patients, all males, had been diagnosed with ASD. The mean verbal IQ was 83.6, while the mean performance IQ was 91.4. For all patients, I used the template tract ROI method to obtain microstructural data.

No microstructural variable was a significant predictor of either verbal IQ or performance – verbal IQ split. AF MD was the closest to reaching statistical significance, but was not a

significant predictor of verbal IQ after correction for multiple comparisons ($p = 0.041$). Sex was a significant predictor of verbal IQ in the models for the AF, SLF, and ILF ($p < 0.004$). Of the microstructural variable predictors other than AF MD, only AF FA Laterality ($p = 0.107$ for performance – verbal IQ split) and AF FA ($p = 0.099$ for verbal IQ and $p = 0.107$ for performance – verbal IQ split) neared the threshold of significance for prediction before correction for multiple comparisons.

4. Discussion

4.1 Major Findings

Results from the traditional tractography approach showed large differences in TSC patients with ASD, particularly in the AF. As previously noted, the AF is the best-characterized brain language pathway, although evidence linking specific changes in its microstructure (as opposed to gross lesions) with language outcomes remains somewhat limited. The AF MD (figure 8) showed a clear separation of the three groups, with a MD increase in TSC patients with ASD relative to both controls and TSC patients without ASD. Similarly, the AF FA (figure 7) for TSC patients with ASD was below the FA for both controls and TSC patients without ASD.

Unlike the UF, which is likely involved in socio-emotional processing rather than language, each of the putative language pathways (SLF, ILF, IFOF) also showed significant differences depending on group status. The SLF MD, in particular, showed aberrant development with increasing age, with both TSC patients with ASD and their counterparts without ASD exhibiting increased MD relative to control subjects. The ILF and IFOF appeared to have a completely different developmental trajectory in TSC patients with ASD than control subjects and TSC

patients without ASD, although the results may be an artifact of the cross-sectional study design. In particular, TSC patients with ASD had nearly level ILF FA and MD, as well as IFOF FA and MD across the range of ages. Although the rates of development can vary among different tracts, with some exhibiting early myelination, control patients and TSC patients without ASD exhibited the expected developmental increase in FA and decrease in MD (Dubois, Dehaene-Lambertz et al. 2008).

The AF results were clearly the strongest, but the problem of missing data makes interpretation somewhat more challenging. Nine of the forty-two controls and nine of the forty-two patients did not have an identifiable AF with the traditional tractography approach. The challenge of identifying the AF, particularly in the youngest subjects, has frequently been reported (Fletcher, Whitaker et al. 2010; Knaus, Silver et al. 2010; Yeatman, Dougherty et al. 2011). Without better methods for finding the AF, it will remain difficult to study AF and language development in the youngest subjects. In particular, even with data from subjects as young as one year of age, it is not clear if AF changes are due to biology-environment interactions in the first year of life, or due to differences at birth in TSC children. Combining improved methods of AF identification with prospective studies of TSC will be essential.

For the small study predicting verbal IQ and performance – verbal IQ split, the small number of patients made it difficult to identify strong predictors. Most likely by chance, female participants had much higher verbal IQ than male participants. AF MD showed a trend toward predicting verbal IQ ($p = 0.041$), with higher MD associated with lower verbal IQ. The result was not statistically significant after multiple comparisons correction. Prospective studies with a younger and larger group of patients are essential for determining if there is a true relationship.

4.2 Relationship to previous studies

This thesis is the first to study microstructural characteristics of language pathways in TSC. Moreover, it is only the second analysis of TSC brain microstructure of any region that also incorporates clinical neurological outcome, following a recent study on the corpus callosum (Peters, Sahin et al. 2012). Other work on TSC has been unable to examine neurological correlates of neuroimaging findings due to smaller sample sizes. The decreased FA in patients relative to controls—and particularly in patients with ASD—suggests that TSC is associated with impaired tract cohesion in language regions of the brain. Decreased FA indicates poor tract integrity and likely represents diminished compactness of the fiber tracts. For the AF, the developmental trajectories of microstructural variables are similar across groups, but the model suggests that the FA may be significantly different at age one (represented by the intercepts of the log(Age) fits). This difference in early FA appears to be maintained through development, potentially relating to the high prevalence of language deficits in the TSC population. It is also possible that poor language development is actually the cause of the reduced tract integrity in brain language regions of TSC patients.

Similarly, increased MD in patients, particularly those with ASD, suggests impaired maturation of white matter language pathways. Higher MD in the TSC population may be related to incomplete or improper myelination compared to normal controls (Song, Sun et al. 2003) (Song, Sun et al. 2002). Improper or inadequate myelination in TSC is consistent with mouse studies demonstrating reduced myelination in the brains of mice lacking *Tsc1* or *Tsc2* (Meikle, Talos et al. 2007) (Way, McKenna et al. 2009). Mutations in *TSC1* and *TSC2* cause a variety of neural abnormalities in mouse models, including changes in neurofilaments and cell size, as well as dendritic spine density and length. Thus, although hypomyelination may be partly responsible

for the observed increase in MD in TSC patients, more general neuronal dysfunction likely contributes as well.

It is somewhat surprising that changes in the volume of the language pathways were not seen with traditional tractography in patients with TSC. The aberrant development of language pathways in this patient group might be expected to contribute to volume changes as well. Fletcher and colleagues found similar results similar in patients with high-functioning autism. They observed no volume changes with age, and no volume differences between patients with ASD and controls (Fletcher, Whitaker et al. 2010). Some evidence, though, suggests that subjects with typical language activation actually have lower volume of the AF (Knaus, Silver et al. 2010).

These results are consistent with findings of aberrant AF structure in idiopathic ASD. Recent work suggests that the microstructure of the AF is modified in patients with high-functioning ASD compared to age-matched controls, even when controlling for overall white matter microstructure (Fletcher, Whitaker et al. 2010). Patients with ASD are also more likely to have atypical laterality than controls, although there were subjects with atypical laterality in both groups (Knaus, Silver et al. 2010).

4.3 Template tract ROI method

The template tract ROI method allowed the assessment of the structure of regions where language tracts normally develop. Even when tracts are absent with traditional tractograpy (particularly curving tracts like the AF) using the template tract ROI approach allows analysis of regions that likely contain the tract of interest. In some ways, the template tract ROI approach is a form of probabilistic tractography. While the most common algorithms for probabilistic

tractography assign probable regions based on the full diffusion tensor data of a single subject, the template tract ROI method assigns likely regions based on the known developmental regions. The template tract ROI will always find a region, even in patients who are very young (Fletcher, Whitaker et al. 2010) (Yeatman, Dougherty et al. 2011).

In this study, the template tract ROI method gave similar results to the traditional tractography method, while including subjects (nine controls and nine TSC patients in the case of the AF) who could not be included in the traditional analysis. The template tract ROI method verified the traditional tractography finding that AF MD is much higher in TSC patients with ASD than TSC patients without ASD or controls. Surprisingly, though, for the template tract ROI method, the model suggested that patients with ASD actually had a paradoxical increase in MD with age in the region of the brain where the AF normally develops. The results of the template tract ROI method included the youngest subjects diagnosed with ASD, strengthening the relevance of the findings in young TSC patients.

For the AF FA, the traditional tractography method showed a decreased intercept associated with TSC patients with ASD (representing a lower predicted FA at age one). In contrast, the template tract ROI method showed a decreased slope of the LOG(Age) versus FA graph. Thus, the model generated from from the traditional tractography method suggest that patients with ASD have low FA from an early age, although the paucity of data on these patients in our study means that conclusions about this age group require further study. The template tract ROI method may not be as sensitive to differences among the groups in specific language pathways because it analyzes larger developmental regions rather than selected streamlines.

The template tract ROI method also allowed the assessment of FA laterality, because both left-sided and right-sided tract ROIs could be generated for all subjects. In general, the laterality

was similar for the three groups (controls, TSC patients without ASD, and TSC patients with ASD), but patients with ASD showed a small rightward shift relative to both controls and patients without ASD in the ILF and IFOF (figure 9 for ILF). Because the left side of the brain is typically language-dominant, the changes in laterality suggest that patients with ASD may be compensating for poor microstructure in left-sided ILF and IFOF by modifying the structure of the right-sided pathways. Alternatively, the results could suggest that the right side ILF and IFOF FA are relatively normal and only appear improved due to their comparison to reduced values on the left side of ASD patients.

For future prospective studies of TSC patients, the template tract ROI method may be useful to assess AF structure from birth, rather than waiting until the AF has developed sufficiently to use traditional tractography. Further refinement in the template tract ROI method will be necessary to ensure the developmental regions are accurately identified, even in the youngest patients.

4.4 Fractional occupancy method

The fractional occupancy method aims to improve the assessment of white matter tract volume and tract-based spatial statistics. Particularly when calculating the volume of a white matter tract, the volume of other white matter tracts in the same voxel is typically ignored. To improve volume calculations, the fractional occupancy method weights both the volume of each voxel (when calculating the overall volume of a tract) and the FA or MD of each voxel (when calculating tract-based spatial statistics) by the occupancy of the tract of interest within each voxel. The fractional occupancy method also uses a white matter segmentation to automatically exclude voxels that are primarily gray matter or CSF. Including voxels that are primarily gray matter would artificially increase the overall volume and decrease FA and MD. Including voxels of CSF would artificially increase volume and MD, as well as decreasing FA.

In general, the results from the fractional occupancy method were similar to the results of the traditional tractography method. Both methods showed major differences in AF FA and AF MD when comparing TSC patients with ASD and controls, but the differences were less pronounced for the fractional occupancy method when comparing TSC patients without ASD and controls. The areas at the margins of the calculated arcuate fasciulus are given reduced significance in the fractional occupancy method, meaning that the differences between groups may be amplified less than with the traditional tractography method. Instead, in TSC patients, the central arcuate fasciculus may be relatively preserved, while the border regions may be those that lack compactness. It is these edge regions that are counted less in the calculcations performed with the fractional occupancy method.

With the fractional occupancy method, none of the tracts studied showed significant volume changes based on diagnosis, although the IFOF showed a trend toward decreased volume with age in patients with ASD relative to controls (figure 9; $p = 0.008$). The fractional occupancy did show the wide variability of tract volumes in different patients. Looking at more regions of the brain and assessing the volume with a larger group of young subjects may allow the identification of tracts with different volumes. Intuitively, the fractional occupancy approach makes more sense than assessing volume with the traditional tractography approach, specifically because it forces the sum of all independent tract volumes in the brain to equal the volume of all white matter in the brain. In contrast, summing the volumes of all independent tracts with the traditional tractography approach would lead to a volume several times larger than the total white matter volume.

The fractional occupancy method remains promising for assessing both statistics and volume, although better tractography techniques are required to profit from its advantages. Future work

with multiple tensors in each voxel, as well as multiple-compartment models (assessing free water and gray matter fractions) will allow the fractional occupancy method to make better predictions of both microstructural values and volume.

4.5 Limitations

There are several limitations to the current study. Most importantly, while the study highlights a variety of DTI microstructural measures, it does not take into account important clinical variables that may lead to autism in TSC patients. Ideally, future work would consider both important clinical findings (e.g early seizures and genetics, as shown by Numis *et al.*) and compare them to the relevance of neuroimaging data. Predicting those patients at risk for poor sociobehavioral outcomes will likely require a multi-pronged approach, including imaging, genetics, and clinical findings. Such prospective studies are underway.

In terms of data collection, the study suffered from the challenges of a dataset that was collected over a period of years. Although all the data were collected with the same diffusion sequence and analyzed with the same pipeline, it is possible that subtle differences in patient motion could lead to lower-quality data in patients with TSC and could thereby affect the conclusions (Yendiki, Koldewyn et al. 2013). It should be noted that to prepare the data for diffusion tensor calculation, robust motion and distortion correction was performed, although this does not eliminate the possibility of bias due to increased head motion in one group.

Another limitation to this study is the absence of information regarding cortical tubers in patients with TSC and their relationship to the microstructural changes identified in this study. Large tubers that completely obstructed language tracts would not have changed the results for the traditional tractography and fractional occupancy methods because the language tract data

would have been treated as missing. Large tubers may have affected the template tract ROI method data, however. Small tubers could have affected the data from all three methods. Future studies that incorporate automated tuber detection will improve our understanding of the contributions of microstructural changes in normal appearing white matter versus language region tuber burden to poor language development in TSC.

This study also lacked handedness data for the patients and controls, meaning that differences in handedness could have explained some of the differences among the three groups (controls, patients without ASD, and patients with ASD). It should be noted that there is not a one-to-one relationship between laterality in the brain and handedness, but left-handed subjects are less likely to have clear laterality in brain language areas than are right-handed subjects (Johnson, Yeatman et al. 2013). Confirmation of the findings in the right SLF and right ILF (traditional tractography) as well as the right AF (template tract ROI method) suggests that the differences likely do not arise simply due to differences in handedness among the groups. In particular, if differences in handedness were the main cause of the findings, we would expect the findings on the right side of the brain to disappear, or even be reversed. In contrast, the findings in the few tracts examined on the right side of the brain exhibited the same general pattern as those on the left side of the brain. Although the findings on the left side are stronger, the increased separation among groups on the left side may be due to the role of left-sided tracts in language. Figure 11 shows a comparison of the findings on the left side with those on the right.

The study is also limited by its design. Rather than examining patients longitudinally, the study looks at a sample of patients at one point in time, and infers developmental patterns based on that cross-section. Future studies of the developmental trajectory of patients with TSC will require prospective design. Cross-sectional studies, particularly small ones, may show findings (particularly ‘developmental findings’) due to difficult-to-quantify differences between young and

old patients in the study, or even young and old controls. Unfortunately, due to the relative rarity of TSC, cross-sectional studies remain the most accessible, despite their limitations.

The new methods present their own drawbacks. The template tract ROI method, although it allows detailed assessment of very young patients, likely smoothens differences among groups, because it considers the entire region near a likely tract, rather than just the tract itself. Similar challenges are found with probabilistic tractography, which also risks including regions around the tract of interest in addition to the tract itself. Figure 10 shows a comparison of the AF models based on which analysis method was used.

In this analysis, the fractional occupancy method for microstructural variables did not provide different results, in general, from traditional tractography. The fractional occupancy method does allow more logical assessment of volume, and may improve the calculation of microstructural values for tracts that pass through crossing-regions (like the AF). The fractional occupancy method requires accurate white matter segmentation, though, which proves difficult in the youngest subjects (Weisenfeld and Warfield 2009). Most tracts in young subjects lack adult concentrations of myelin, making identification of the white matter particularly challenging.

A final limitation concerns the neuropsychiatric analysis. Several different IQ tests were used in the prediction of verbal IQ, because the patients each received a different battery of tests based on the clinical judgment of Dr. Rachel Hundley. Because patients received different IQ tests (although the IQ tests had identical distributions), differences in verbal IQ may have resulted from the changes in IQ test used, rather than true differences in verbal IQ.

4.6 Future studies

This work suggests that future studies predicting ASD phenotype and language outcome in TSC patients should examine the contribution of neuroimaging data. Many questions remain. The relationship between ASD and seizures, as well as seizures in TSC and microstructure in TSC remains difficult to disentangle. Further work examining the importance of the age of seizure onset and seizure frequency on microstructure in TSC patients will help establish the relationship. Given the small number of young patients in this study, it is also difficult to draw conclusions about the youngest population. Because it is young patients in whom intervention would most likely be beneficial, future studies will need to start at a young age (likely before ASD diagnosis is even possible) and have a prospective design.

Future studies will also include additional clinical variables, including medications used, and improved matching for IQ. Full ADOS and language scores in all patients will allow more accurate assessment of microstructural variables for prediction of language outcomes. Finally, automated techniques for assessing tuber load will help determine the true relationship between tuber location and density and language outcomes.

5. Conclusions

Our findings demonstrate that controls, TSC patients without ASD, and TSC patients with ASD have significantly different AF microstructure. The differences are particularly pronounced when comparing controls and TSC patients with ASD. Moreover, there was a trend toward AF MD correlation with verbal IQ in a small sample of patients. Thus, AF MD may prove to be a useful marker for informing early pharmaceutical and behavior intervention, although the question requires significant additional investigation (Sahin, Miller et al. 2011). Recent work has also correlated ASD in TSC to early seizure activity and more frequent seizures (Numis, Major et al.

2011). It is unclear, though, if ASD and frequent/early seizures have a common cause, or whether the seizures themselves may cause autistic symptoms directly.

The results from this study, particularly the model suggesting poor AF microstructural integrity from age one, indicate a possible relationship among aberrant white matter microstructural integrity, poor cognitive function, early seizures, and ASD. While the group of ASD patients in general is heterogeneous, studying TSC patients can help shed light on patients with ASD caused by genetic defects in TSC1/2 and genes in related molecular pathways (Tsai and Sahin 2011).

Acknowledgements

Thank you first to Mustafa Sahin and Simon Warfield for guiding me, particularly in the design of my project. Without their combination of TSC knowledge and imaging expertise, this project would not have been possible. I also particularly appreciate the help and guidance of Benoit Scherrer. His knowledge of the pre-processing and tractography algorithms and his willingness to critique my ideas helped me complete a much better thesis. Thank you to Ralph Suarez, for helping me adapt his new ROI mapping technique to the language pathways in the brain. Jurriaan Peters, Shefali Jeste, Rachel Hundley, and Vanessa Vogel-Farley helped provide clinical perspective and also performed ADOS testing on a number of the TSC patients. Finally, thank you to the Sahin and Warfield labs for helping me with good discussions and critiques and generally welcoming me!

References

(2007). "Prevalence of autism spectrum disorders--autism and developmental disabilities monitoring network, 14 sites, United States, 2002." MMWR. Surveillance summaries : Morbidity and mortality weekly report. Surveillance summaries / CDC **56**(1): 12-28.

Alexander, A. L., K. M. Hasan, et al. (2001). "Analysis of partial volume effects in diffusion-tensor MRI." Magnetic resonance in medicine : official journal of the Society of Magnetic Resonance in Medicine / Society of Magnetic Resonance in Medicine **45**(5): 770-780.

Alexander, A. L., J. E. Lee, et al. (2007). "Diffusion tensor imaging of the corpus callosum in Autism." NeuroImage **34**(1): 61-73.

Ameis, S. H., J. Fan, et al. (2011). "Impaired structural connectivity of socio-emotional circuits in autism spectrum disorders: a diffusion tensor imaging study." PloS one **6**(11): e28044.

Aoki, Y., O. Abe, et al. (2013). "Comparison of white matter integrity between autism spectrum disorder subjects and typically developing individuals: a meta-analysis of diffusion tensor imaging tractography studies." Molecular autism **4**(1): 25.

Arsigny, V., P. Fillard, et al. (2006). "Log-Euclidean metrics for fast and simple calculus on diffusion tensors." Magnetic resonance in medicine : official journal of the Society of Magnetic Resonance in Medicine / Society of Magnetic Resonance in Medicine **56**(2): 411-421.

Arulrajah, S., G. Ertan, et al. (2009). "Magnetic resonance imaging and diffusion-weighted imaging of normal-appearing white matter in children and young adults with tuberous sclerosis complex." Neuroradiology **51**(11): 781-786.

Asano, E., D. C. Chugani, et al. (2001). "Autism in tuberous sclerosis complex is related to both cortical and subcortical dysfunction." Neurology **57**(7): 1269-1277.

Baskin, H. J., Jr. (2008). "The pathogenesis and imaging of the tuberous sclerosis complex." Pediatric radiology **38**(9): 936-952.

Bastin, M. E., S. Munoz Maniega, et al. (2010). "Quantifying the effects of normal ageing on white matter structure using unsupervised tract shape modelling." NeuroImage **51**(1): 1-10.

Bernal, B., G. Rey, et al. (2010). "Agenesis of the arcuate fasciculi in congenital bilateral perisylvian syndrome: a diffusion tensor imaging and tractography study." Archives of neurology **67**(4): 501-505.

Buchsbaum, M. S., C. Y. Tang, et al. (1998). "MRI white matter diffusion anisotropy and PET metabolic rate in schizophrenia." Neuroreport **9**(3): 425-430.

Catani, M., D. K. Jones, et al. (2005). "Perisylvian language networks of the human brain." Annals of neurology **57**(1): 8-16.

Catani, M. and M. Thiebaut de Schotten (2008). "A diffusion tensor imaging tractography atlas for virtual in vivo dissections." Cortex; a journal devoted to the study of the nervous system and behavior **44**(8): 1105-1132.

Chu-Shore, C. J., P. Major, et al. (2009). "Cyst-like tubers are associated with TSC2 and epilepsy in tuberous sclerosis complex." Neurology **72**(13): 1165-1169.

Ciccarelli, O., M. Catani, et al. (2008). "Diffusion-based tractography in neurological disorders: concepts, applications, and future developments." Lancet neurology **7**(8): 715-727.

Crino, P. B., K. L. Nathanson, et al. (2006). "The tuberous sclerosis complex." The New England journal of medicine **355**(13): 1345-1356.

de Weijer, A. D., S. F. Neggers, et al. (2011). "Aberrations in the arcuate fasciculus are associated with auditory verbal hallucinations in psychotic and in non-psychotic individuals." Human brain mapping.

Dinstein, I., K. Pierce, et al. (2011). "Disrupted neural synchronization in toddlers with autism." Neuron **70**(6): 1218-1225.

Douek, P., R. Turner, et al. (1991). "MR color mapping of myelin fiber orientation." Journal of computer assisted tomography **15**(6): 923-929.

Dubois, J., G. Dehaene-Lambertz, et al. (2008). "Asynchrony of the early maturation of white matter bundles in healthy infants: quantitative landmarks revealed noninvasively by diffusion tensor imaging." Human brain mapping **29**(1): 14-27.
Duffau, H., P. Gatignol, et al. (2009). "Is the left uncinate fasciculus essential for language? A cerebral stimulation study." Journal of neurology **256**(3): 382-389.
Duffau, H., S. T. Peggy Gatignol, et al. (2008). "Intraoperative subcortical stimulation mapping of language pathways in a consecutive series of 115 patients with Grade II glioma in the left dominant hemisphere." Journal of neurosurgery **109**(3): 461-471.
Fletcher, P. T., R. T. Whitaker, et al. (2010). "Microstructural connectivity of the arcuate fasciculus in adolescents with high-functioning autism." NeuroImage **51**(3): 1117-1125.
Geschwind, N. and W. Levitsky (1968). "Human brain: left-right asymmetries in temporal speech region." Science **161**(3837): 186-187.
Goh, S., D. J. Kwiatkowski, et al. (2005). "Infantile spasms and intellectual outcomes in children with tuberous sclerosis complex." Neurology **65**(2): 235-238.
Grau, V., A. U. Mewes, et al. (2004). "Improved watershed transform for medical image segmentation using prior information." IEEE transactions on medical imaging **23**(4): 447-458.
Groen, W. B., J. K. Buitelaar, et al. (2011). "Pervasive microstructural abnormalities in autism: a DTI study." Journal of psychiatry & neuroscience : JPN **36**(1): 32-40.
Han, J. M. and M. Sahin (2011). "TSC1/TSC2 signaling in the CNS." FEBS letters **585**(7): 973-980.
Hasan, K. M., A. Iftikhar, et al. (2009). "Development and aging of the healthy human brain uncinate fasciculus across the lifespan using diffusion tensor tractography." Brain research **1276**: 67-76.
Hsu, J. L., A. Leemans, et al. (2008). "Gender differences and age-related white matter changes of the human brain: a diffusion tensor imaging study." NeuroImage **39**(2): 566-577.
Hsu, J. L., W. Van Hecke, et al. (2010). "Microstructural white matter changes in normal aging: a diffusion tensor imaging study with higher-order polynomial regression models." NeuroImage **49**(1): 32-43.
Humphrey, A., J. N. Higgins, et al. (2004). "Monozygotic twins with tuberous sclerosis discordant for the severity of developmental deficits." Neurology **62**(5): 795-798.
Jansen, F. E., K. L. Vincken, et al. (2008). "Cognitive impairment in tuberous sclerosis complex is a multifactorial condition." Neurology **70**(12): 916-923.
Jeong, J. W., S. K. Sundaram, et al. (2011). "Aberrant diffusion and geometric properties in the left arcuate fasciculus of developmentally delayed children: a diffusion tensor imaging study." AJNR. American journal of neuroradiology **32**(2): 323-330.
Jeste, S. S., M. Sahin, et al. (2008). "Characterization of autism in young children with tuberous sclerosis complex." Journal of child neurology **23**(5): 520-525.
Johnson, R. T., J. D. Yeatman, et al. (2013). "Diffusion properties of major white matter tracts in young, typically developing children." NeuroImage.
Jones, D. K., M. Catani, et al. (2006). "Age effects on diffusion tensor magnetic resonance imaging tractography measures of frontal cortex connections in schizophrenia." Human brain mapping **27**(3): 230-238.
Jou, R. J., N. Mateljevic, et al. (2011). "Structural neural phenotype of autism: preliminary evidence from a diffusion tensor imaging study using tract-based spatial statistics." AJNR. American journal of neuroradiology **32**(9): 1607-1613.
Karadag, D., H. J. Mentzel, et al. (2005). "Diffusion tensor imaging in children and adolescents with tuberous sclerosis." Pediatric radiology **35**(10): 980-983.
Kim, C. H., C. K. Chung, et al. (2011). "Changes in language pathways in patients with temporal lobe epilepsy: diffusion tensor imaging analysis of the uncinate and arcuate fasciculi." World neurosurgery **75**(3-4): 509-516.
Knaus, T. A., A. M. Silver, et al. (2010). "Language laterality in autism spectrum disorder and typical controls: a functional, volumetric, and diffusion tensor MRI study." Brain and language **112**(2): 113-120.

Krishnan, M. L., O. Commowick, et al. (2010). "Diffusion features of white matter in tuberous sclerosis with tractography." Pediatric neurology **42**(2): 101-106.
Kubicki, M., J. L. Alvarado, et al. (2011). "Stochastic tractography study of Inferior Frontal Gyrus anatomical connectivity in schizophrenia." NeuroImage **55**(4): 1657-1664.
Lai, M. C., M. V. Lombardo, et al. (2011). "A behavioral comparison of male and female adults with high functioning autism spectrum conditions." PloS one **6**(6): e20835.
Lazar, M., D. M. Weinstein, et al. (2003). "White matter tractography using diffusion tensor deflection." Human brain mapping **18**(4): 306-321.
Lebel, C. and C. Beaulieu (2009). "Lateralization of the arcuate fasciculus from childhood to adulthood and its relation to cognitive abilities in children." Human brain mapping **30**(11): 3563-3573.
Lebel, C., L. Walker, et al. (2008). "Microstructural maturation of the human brain from childhood to adulthood." NeuroImage **40**(3): 1044-1055.
Leclercq, D., H. Duffau, et al. (2010). "Comparison of diffusion tensor imaging tractography of language tracts and intraoperative subcortical stimulations." Journal of neurosurgery **112**(3): 503-511.
Makki, M. I., D. C. Chugani, et al. (2007). "Characteristics of abnormal diffusivity in normal-appearing white matter investigated with diffusion tensor MR imaging in tuberous sclerosis complex." AJNR. American journal of neuroradiology **28**(9): 1662-1667.
Mandonnet, E., A. Nouet, et al. (2007). "Does the left inferior longitudinal fasciculus play a role in language? A brain stimulation study." Brain : a journal of neurology **130**(Pt 3): 623-629.
Marchina, S., L. L. Zhu, et al. (2011). "Impairment of speech production predicted by lesion load of the left arcuate fasciculus." Stroke; a journal of cerebral circulation **42**(8): 2251-2256.
Meikle, L., D. M. Talos, et al. (2007). "A mouse model of tuberous sclerosis: neuronal loss of Tsc1 causes dysplastic and ectopic neurons, reduced myelination, seizure activity, and limited survival." The Journal of neuroscience : the official journal of the Society for Neuroscience **27**(21): 5546-5558.
Mori, S., B. J. Crain, et al. (1999). "Three-dimensional tracking of axonal projections in the brain by magnetic resonance imaging." Annals of neurology **45**(2): 265-269.
Noriuchi, M., Y. Kikuchi, et al. (2010). "Altered white matter fractional anisotropy and social impairment in children with autism spectrum disorder." Brain research **1362**: 141-149.
Numis, A. L., P. Major, et al. (2011). "Identification of risk factors for autism spectrum disorders in tuberous sclerosis complex." Neurology **76**(11): 981-987.
Oouchi, H., K. Yamada, et al. (2007). "Diffusion anisotropy measurement of brain white matter is affected by voxel size: underestimation occurs in areas with crossing fibers." AJNR. American journal of neuroradiology **28**(6): 1102-1106.
Osborne, J. P., A. Fryer, et al. (1991). "Epidemiology of tuberous sclerosis." Annals of the New York Academy of Sciences **615**: 125-127.
Pardini, M., M. Elia, et al. (2011). "Long-term Cognitive and Behavioral Therapies, Combined with Augmentative Communication, are Related to Uncinate Fasciculus Integrity in Autism." Journal of autism and developmental disorders.
Pasternak, O., N. Sochen, et al. (2009). "Free water elimination and mapping from diffusion MRI." Magnetic resonance in medicine : official journal of the Society of Magnetic Resonance in Medicine / Society of Magnetic Resonance in Medicine **62**(3): 717-730.
Peng, S. S., W. T. Lee, et al. (2004). "Cerebral diffusion tensor images in children with tuberous sclerosis: a preliminary report." Pediatric radiology **34**(5): 387-392.
Peters, J. M., M. Sahin, et al. (2012). "Loss of white matter microstructural integrity is associated with adverse neurological outcome in tuberous sclerosis complex." Academic radiology **19**(1): 17-25.
Pfefferbaum, A., E. Adalsteinsson, et al. (2003). "Replicability of diffusion tensor imaging measurements of fractional anisotropy and trace in brain." Journal of magnetic resonance imaging : JMRI **18**(4): 427-433.
Piao, C., A. Yu, et al. (2009). "Cerebral diffusion tensor imaging in tuberous sclerosis." European journal of radiology **71**(2): 249-252.

Powell, H. W., G. J. Parker, et al. (2006). "Hemispheric asymmetries in language-related pathways: a combined functional MRI and tractography study." NeuroImage **32**(1): 388-399.
Pugliese, L., M. Catani, et al. (2009). "The anatomy of extended limbic pathways in Asperger syndrome: a preliminary diffusion tensor imaging tractography study." NeuroImage **47**(2): 427-434.
Qiu, D., L. H. Tan, et al. (2011). "Lateralization of the arcuate fasciculus and its differential correlation with reading ability between young learners and experienced readers: a diffusion tensor tractography study in a Chinese cohort." Human brain mapping **32**(12): 2054-2063.
Reese, T. G., O. Heid, et al. (2003). "Reduction of eddy-current-induced distortion in diffusion MRI using a twice-refocused spin echo." Magnetic resonance in medicine : official journal of the Society of Magnetic Resonance in Medicine / Society of Magnetic Resonance in Medicine **49**(1): 177-182.
Ridler, K., J. Suckling, et al. (2007). "Neuroanatomical correlates of memory deficits in tuberous sclerosis complex." Cerebral cortex **17**(2): 261-271.
Roach, E. S., F. J. DiMario, et al. (1999). "Tuberous Sclerosis Consensus Conference: recommendations for diagnostic evaluation. National Tuberous Sclerosis Association." Journal of child neurology **14**(6): 401-407.
Ruiz-Alzola, J., C. F. Westin, et al. (2002). "Nonrigid registration of 3D tensor medical data." Medical image analysis **6**(2): 143-161.
Sahin, M., I. Miller, et al. (2011). "Pediatric epileptology." Epilepsy & behavior : E&B **22**(1): 32-37.
Sahyoun, C. P., J. W. Belliveau, et al. (2010). "White matter integrity and pictorial reasoning in high-functioning children with autism." Brain and cognition **73**(3): 180-188.
Saporta, A. S., A. Kumar, et al. (2011). "Arcuate fasciculus and speech in congenital bilateral perisylvian syndrome." Pediatric neurology **44**(4): 270-274.
Saur, D., B. W. Kreher, et al. (2008). "Ventral and dorsal pathways for language." Proceedings of the National Academy of Sciences of the United States of America **105**(46): 18035-18040.
Schmithorst, V. J. and W. Yuan (2010). "White matter development during adolescence as shown by diffusion MRI." Brain and cognition **72**(1): 16-25.
Simao, G., C. Raybaud, et al. (2010). "Diffusion tensor imaging of commissural and projection white matter in tuberous sclerosis complex and correlation with tuber load." AJNR. American journal of neuroradiology **31**(7): 1273-1277.
Song, S. K., S. W. Sun, et al. (2003). "Diffusion tensor imaging detects and differentiates axon and myelin degeneration in mouse optic nerve after retinal ischemia." NeuroImage **20**(3): 1714-1722.
Song, S. K., S. W. Sun, et al. (2002). "Dysmyelination revealed through MRI as increased radial (but unchanged axial) diffusion of water." NeuroImage **17**(3): 1429-1436.
Suarez, R. O., O. Commowick, et al. (2011). "Automated delineation of white matter fiber tracts with a multiple region-of-interest approach." NeuroImage.
Thiebaut de Schotten, M., D. H. Ffytche, et al. (2011). "Atlasing location, asymmetry and inter-subject variability of white matter tracts in the human brain with MR diffusion tractography." NeuroImage **54**(1): 49-59.
Tsai, P. and M. Sahin (2011). "Mechanisms of neurocognitive dysfunction and therapeutic considerations in tuberous sclerosis complex." Current opinion in neurology **24**(2): 106-113.
Upadhyay, J., K. Hallock, et al. (2008). "Diffusion tensor spectroscopy and imaging of the arcuate fasciculus." NeuroImage **39**(1): 1-9.
Vos, S. B., D. K. Jones, et al. (2011). "Partial volume effect as a hidden covariate in DTI analyses." NeuroImage **55**(4): 1566-1576.
Wakana, S., H. Jiang, et al. (2004). "Fiber tract-based atlas of human white matter anatomy." Radiology **230**(1): 77-87.
Walz, N. C., A. W. Byars, et al. (2002). "Supratentorial tuber location and autism in tuberous sclerosis complex." Journal of child neurology **17**(11): 830-832.
Warfield, S. K., K. H. Zou, et al. (2004). "Simultaneous truth and performance level estimation (STAPLE): an algorithm for the validation of image segmentation." IEEE transactions on medical imaging **23**(7): 903-921.

Way, S. W., J. McKenna, 3rd, et al. (2009). "Loss of Tsc2 in radial glia models the brain pathology of tuberous sclerosis complex in the mouse." Human molecular genetics **18**(7): 1252-1265.
Weisenfeld, N. I. and S. K. Warfield (2009). "Automatic segmentation of newborn brain MRI." NeuroImage **47**(2): 564-572.
Wilson, B. J., S. K. Sundaram, et al. (2011). "Abnormal language pathway in children with Angelman syndrome." Pediatric neurology **44**(5): 350-356.
Winterkorn, E. B., M. B. Pulsifer, et al. (2007). "Cognitive prognosis of patients with tuberous sclerosis complex." Neurology **68**(1): 62-64.
Wong, A. M., H. S. Wang, et al. (2013). "Cerebral diffusion tensor MR tractography in tuberous sclerosis complex: correlation with neurologic severity and tract-based spatial statistical analysis." AJNR. American journal of neuroradiology **34**(9): 1829-1835.
Wong, V. and P. L. Khong (2006). "Tuberous sclerosis complex: correlation of magnetic resonance imaging (MRI) findings with comorbidities." Journal of child neurology **21**(2): 99-105.
Yeatman, J. D., R. F. Dougherty, et al. (2011). "Anatomical properties of the arcuate fasciculus predict phonological and reading skills in children." Journal of cognitive neuroscience **23**(11): 3304-3317.
Yendiki, A., K. Koldewyn, et al. (2013). "Spurious group differences due to head motion in a diffusion MRI study." NeuroImage.

Tables, figures, and supplementary figures:

TSC Basics	
gene mutation:	*TSC1* or *TSC2*
mode of inheritance:	autosomal dominant
incidence at birth:	approximately 1 in 5800
symptoms	
neurologic:	epilepsy, autism, tubers
renal:	angiomyolipomas
cardiac:	rhabdomyomas
pulmonary:	lymphangioleiomyomatosis
dermatologic:	small bumps or white spots

Table I: Basic facts about tuberous sclerosis complex (TSC). See the text for a more detailed description of symptoms and their expressivity in TSC. Source: Crino, 2006.

Diffusion-weighted MRI Findings in TSC

Finding:	*Source:*
Increased ADC and reduced FA in tubers	Peng, 2004; Karadag, 2005; Piao, 2009
Decreased subcortical gray matter	Ridler, 2007
Increased MD and reduced FA in white matter	Makki, 2007; Arulrajah, 2009; Krishnan, 2010; Simao, 2010
White matter abnormalities correlate with ASD	Peters, 2012; this thesis

Table II: Diffusion-weighted MRI findings in TSC. Diffusion-weighted MRI shows a variety of abnormalities in TSC. This thesis contributes to the understanding of white matter abnormalities associated with ASD in TSC. See the text for a more detailed description of the findings.

Microstructural Variable	Expression	Interpretation
Fractional Anisotropy	$FA = \sqrt{\frac{3}{2}}\sqrt{\frac{(\lambda_1 - \hat{\lambda}) + (\lambda_2 - \hat{\lambda}) + (\lambda_3 - \hat{\lambda})}{\lambda_1^2 + \lambda_2^2 + \lambda_3^2}}$	Directionality of the diffusion (unitless)
Mean Diffusivity	$MD = \frac{\lambda_1 + \lambda_2 + \lambda_3}{3}$	Average diffusion rate (m^2 / s)
Axial Diffusivity	$AD = \lambda_1$	Diffusion rate in the principal direction (m^2 / s)
Radial Diffusivity	$RD = \frac{\lambda_2 + \lambda_3}{2}$	Diffusion rate perpendicular to the principal direction (m^2 / s)

Table III: Microstructural variables in DTI research. Expression for and interpretation of each microstructural variable commonly-used in DTI studies.

Putative Language Pathways in the Human Brain

Name	*Abbreviation*	*Lobes Connected*	*Electrostimulation Deficit*	*DTI Findings*	*Sources*
Superior Longitudinal Fasciculus	SLF	Parietal to Frontal	Phonological disturbances	Altered in autism	Duffau, 2008; Jou, 2011
Arcuate Fasciculus	AF	Temporal to Frontal	Phonological paraphasia	Correlated with language scores, disease in ASD, schizophrenia, Angelman's	Mandonnet, 2007; Duffau, 2008; Leclercq, 2010; Yeatman, 2011; Lebel, 2009; Qiu, 2011; Marchina, 2011; de Weijer, 2011; Wilson, 2011
Inferior Longitudinal Fasciculus	ILF	Occipital to Temporal	None	Right ILF altered in autism	Mandonnet, 2007; Ameis, 2011
Uncinate Fasciclus	UF	Temporal to Frontal	None	Correlated with behavioral improvements in ASD	Duffau, 2009; Kim, 2011; Pardini, 2011; Pugliese, 2011
Inferior Fronto-occipital Fasciculus	IFOF	Occipital to Frontal	Semantic paraphasia	Altered in autism	Duffau, 2008; Leclercq, 2010; Jou, 2011

Table IV: Putative language pathways in the human brain. Basic information on each putative language pathway studied for this thesis. Of note, the UF is more likely a multi-hemisphere association pathway related to socio-emotional processing rather than a language pathway. Electrostimulation deficit refers to the deficit observed upon intraoperative stimulation of the tract. More detail about the DTI findings can be found in the main text.

Methods Comparison

Name	Streamlines	Voxel statistics	Advantage	Disadvantages
Traditional Tractography	subjects	discrete	easy to compare to literature findings	crossing fibers ignored; some data missing
Template Tract ROI	templates	discrete	generates statistics for all subjects	no comparator studies; smoothes individual variability
Fractional Occupancy	subjects	fractional	compensates for crossing fibers	no comparator studies; some data missing

Table V: A comparison of the methods used in this thesis. Streamlines indicates in which subjects streamlines were generated. Voxel statistics shows how each method treated voxels in the statistical analysis. More detail about each method can be found in the main text.

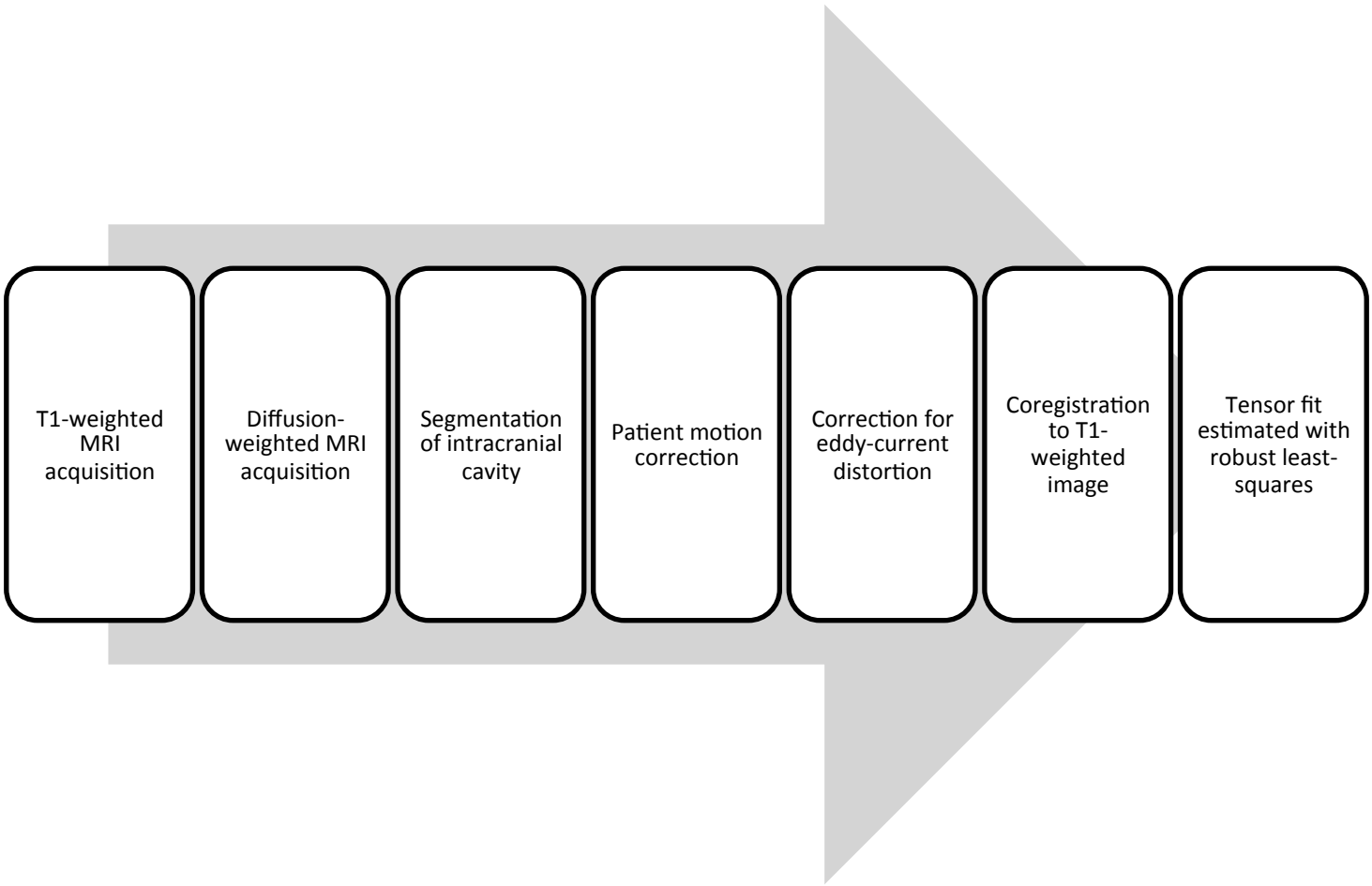

Figure 1: Steps in pre-processing the data for analysis. Each control and patient went through an automated pre-processing pipeline developed by Dr. Benoit Scherrer in the CRL.

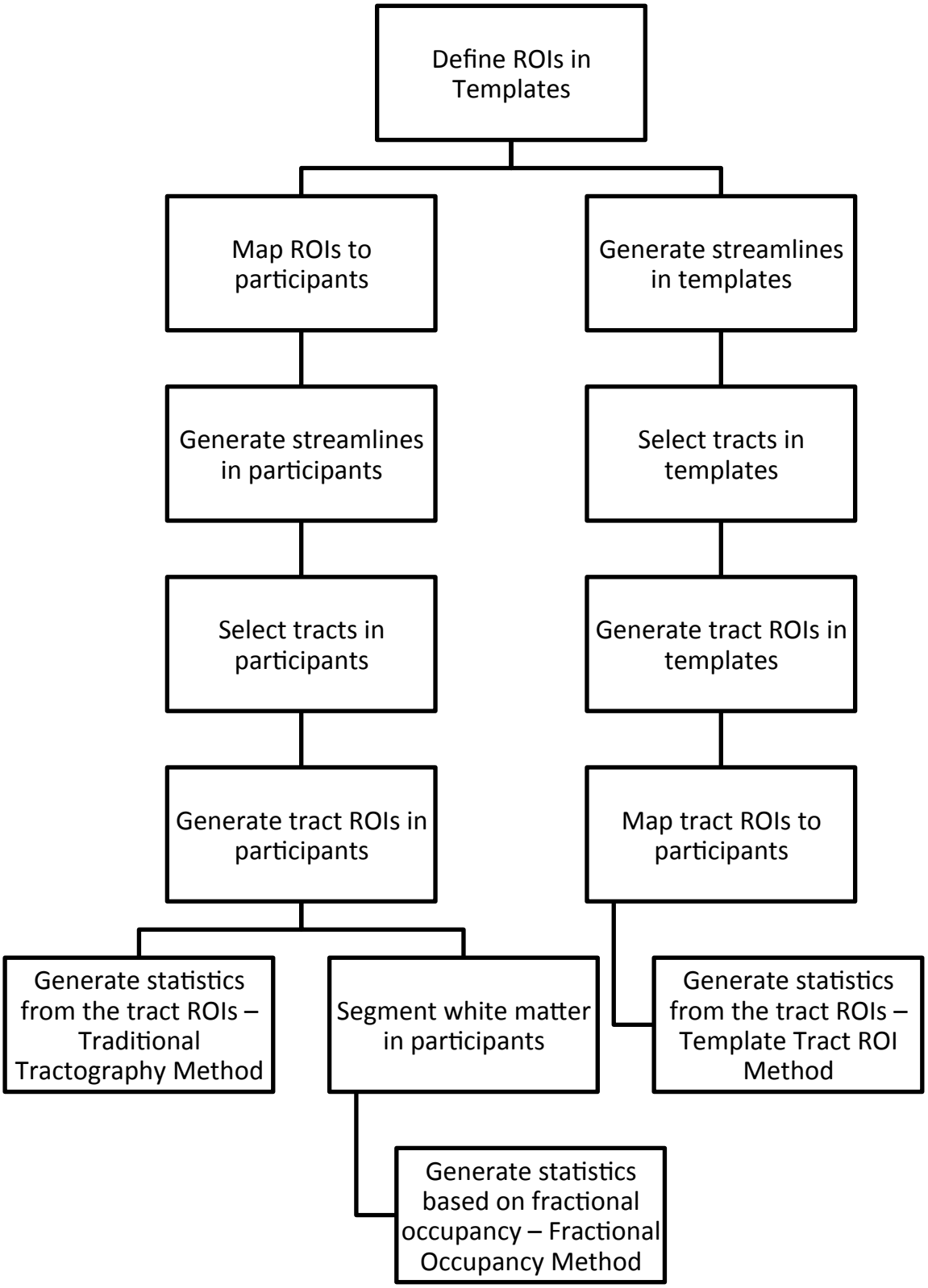

Figure 2: Schematic showing the analysis strategy for each of the three methods. The traditional tractography and fractional occupancy methods use the same strategy for generation of ROIs, streamlines, and tract ROIs, but differ in the analysis of the tract ROIs. The template tract ROI method generates streamlines in the templates, and maps tract ROIs from the templates to the TSC patients and controls in this study.

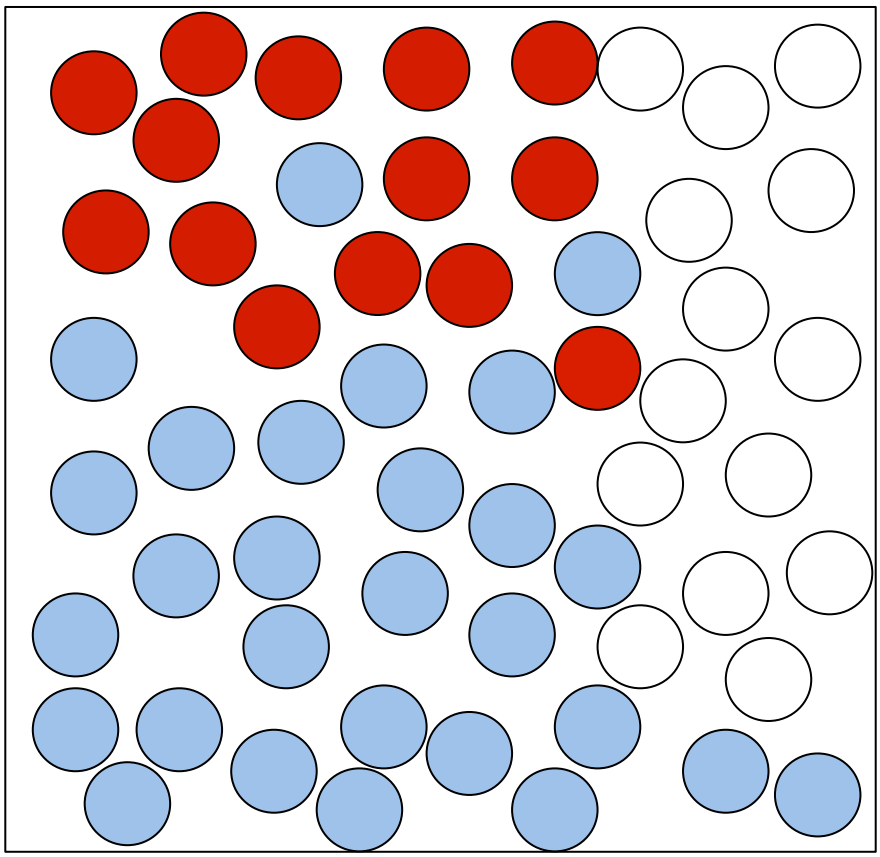

Figure 3: A two-dimensional representation of a voxel shows streamlines that are part of the arcuate fasciculus (in red), superior longitudinal fasciculus (in light blue), and those that are part of other tracts (in white). With the traditional tractography method of determining the volume, this voxel would contribute its entire volume to the arcuate fasciculus and its entire volume to the superior longitudinal fasciculus. With the fractional occupancy method, the volume of a tract within a voxel is instead proportional to the fractional occupancy of its streamlines. In this case, the arcuate fasciculus takes up 14/56 = 1/4 of the voxel and the superior longitudinal fasciculus comprises 28/56 = 1/2 of the voxel.

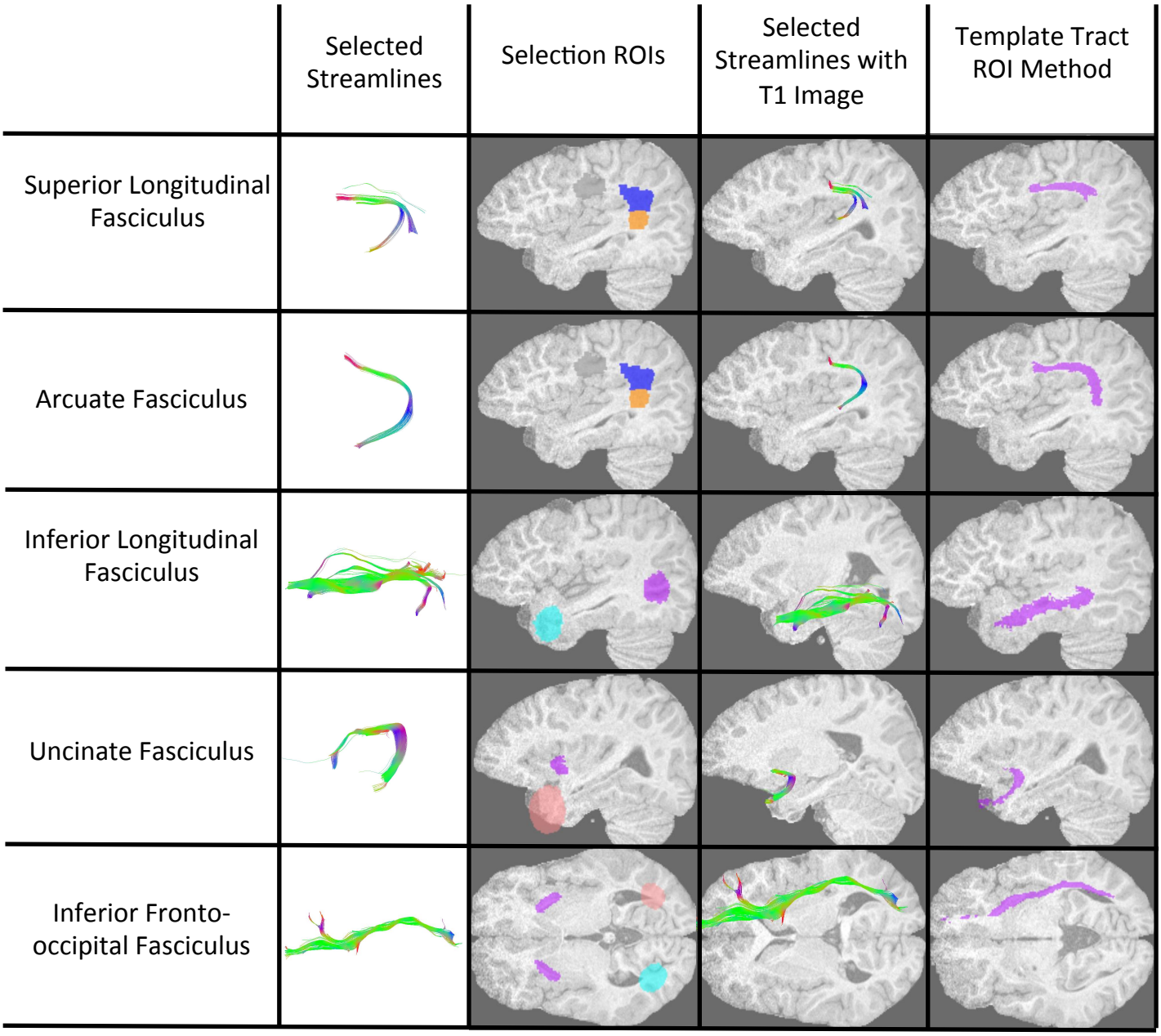

Figure 4: Regions and streamlines for a TSC patient with ASD. Selected streamlines shows the shape of each selected tract (both by itself and overlaid on the T1 image), selection ROIs the regions used to select those streamlines, and template tract ROI method the region analyzed for the template tract ROI method.

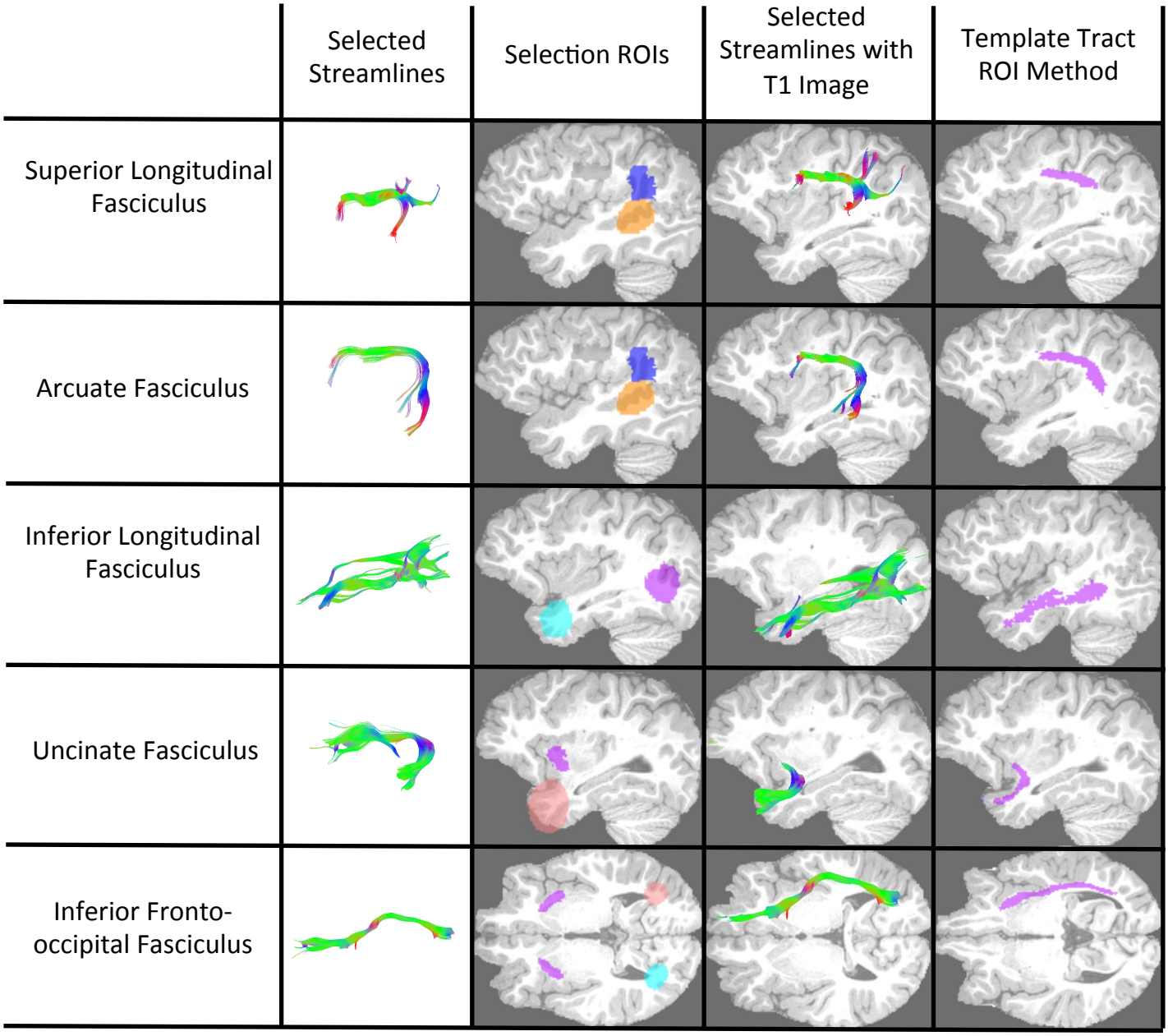

Figure 5: Regions and streamlines for a TSC patient without ASD. Selected streamlines shows the shape of each selected tract (both by itself and overlaid on the T1 image), selection ROIs regions used to select those streamlines, and template tract ROI method the region analyzed for the template tract ROI method.

	Selected Streamlines	Selection ROIs	Selected Streamlines with T1 Image	Template Tract ROI Method
Superior Longitudinal Fasciculus	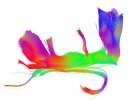	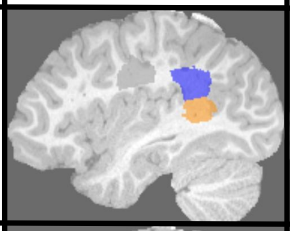	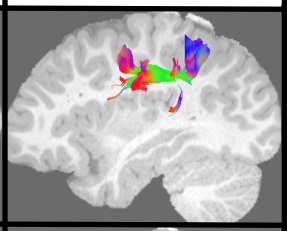	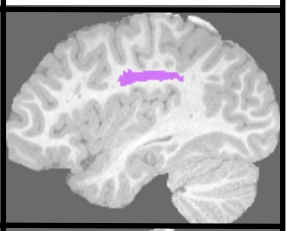
Arcuate Fasciculus	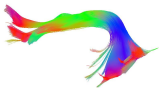	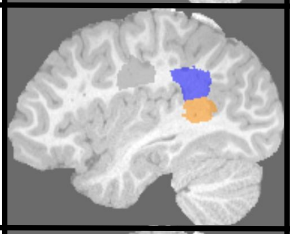	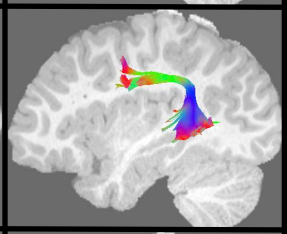	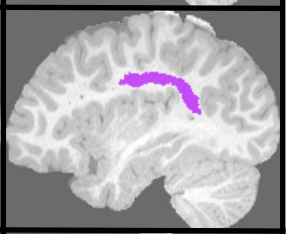
Inferior Longitudinal Fasciculus	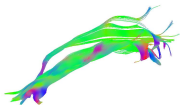	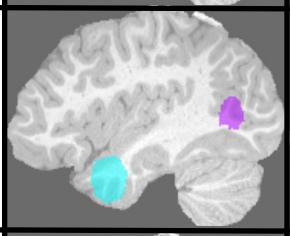	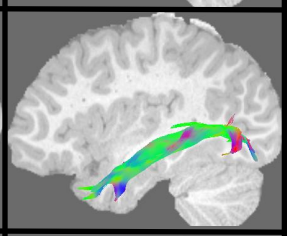	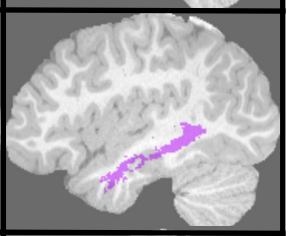
Uncinate Fasciculus	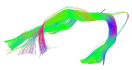	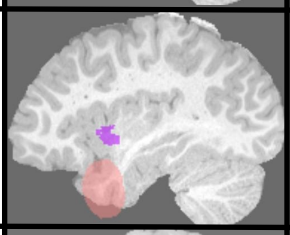	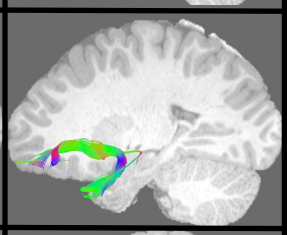	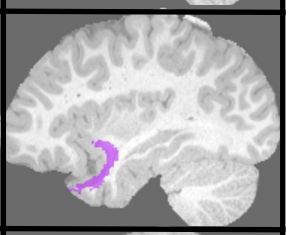
Inferior Fronto-occipital Fasciculus	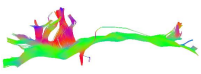	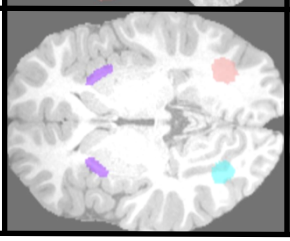	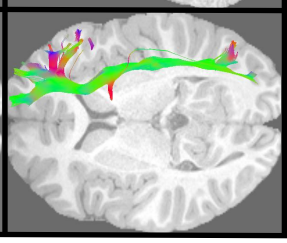	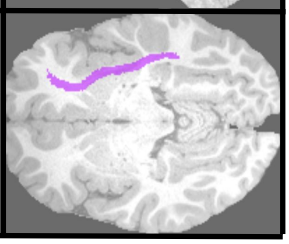

Figure 6: Regions and streamlines for a control subject. Selected streamlines shows the shape of each selected tract (both by itself and overlaid on the T1 image), selection ROIs the regions used to select those streamlines, and template tract ROI method the region analyzed for the template tract ROI method.

	(constant)	LOG(Age)	Sex	Patients without ASD	Patients with ASD	Patients without ASD x LOG(Age)	Patients with ASD x LOG(Age)	R^2
SLF FA	0.367	0.083*		-0.019	-0.049*			0.382
SLF MD	8.93E-04	-0.000118*				3.56E-05	8.08E-05*	0.433
AF FA	0.383	0.079*		-0.025	-0.075* ‡			0.401
AF MD	8.97E-04	-1.25E-04*		3.39E-05	1.28E-04* ‡			0.503
AF AD	1.25E-03	8.05E-05*		3.23E-05	1.11E-04* ‡			0.342
AF RD	7.20E-04	-1.47E-04*		3.46E-05	1.37E-04* ‡			0.508
ILF FA	0.307	0.134*			0.141*		-0.185* ‡	0.501
ILF MD	9.94E-04	-1.54E-04*			-1.18E-04*		2.13E-04* ‡	0.547
UF FA	0.319	0.067*	-0.019					0.382
UF MD	9.62E-04	-1.26E-04*						0.617
IFOF FA	0.348	0.131*			0.123		-0.162*	0.492
IFOF MD	1.00E-03	-1.59E-04*			-1.61E-04		1.98E-04	0.409
Right SLF MD	9.22E-04	-1.40E-04*				2.77E-05	6.90E-05*	0.393
Right ILF MD	9.67E-04	-1.35E-04*		2.84E-05			8.45E-05*	0.518
Age < 10 AF FA	0.353	0.118*		-0.030	-0.062			0.368
Age < 10 AF MD	9.33E-04	-1.78E-04*		4.72E-05	1.06E-04			0.403

for comparisons to controls: * $p < 0.003$
for comparisons to patients without ASD: ‡ $p < 0.003$

Table VI: Regression models for predicting microstructural variables with the traditional tractography method. Entries for each predictor variable refer to their associated β values in the regression model. Predictors marked "NS" did not improve the adjusted R-squared value when added to the model. p-values refer to the significance of the predictor in the model.

	(constant)	LOG(Age)	Sex	Patients without ASD	Patients with ASD	Patients without ASD x LOG(Age)	Patients with ASD x LOG(Age)	R^2
SLF FA	0.323	0.109*		-0.030			-0.070* ‡	0.448
SLF MD	8.94E-04	-1.26E-04*			-8.30E-05	3.30E-05	1.46E-04	0.311
AF FA	0.332	0.102*		-0.024			-0.071* ‡	0.478
AF MD	8.98E-04	-1.24E-04*		4.00E-05	-1.30E-04		2.32E-04* ‡	0.344
ILF FA Laterality	0.126				0.134*			0.127
ILF FA	0.305	0.113*					-0.085* ‡	0.520
ILF MD	9.56E-04	-1.40E-04*		5.56E-05	-2.38E-04		3.82E-04* ‡	0.262
UF Laterality	-0.060	0.092*			-0.040			0.138
UF FA	0.248	0.068*					-0.031	0.314
UF MD	9.71E-04	-1.18E-04*			4.13E-05			0.316
IFOF Laterality	0.079				-0.106*			0.129
IFOF FA	0.360	0.094*					-0.080* ‡	0.430
IFOF MD	9.82E-04	-1.36E-04*					1.92E-04* ‡	0.267
Right AF MD	8.77E-04	-1.09E-04*		3.88E-05*			8.93E-05* ‡	0.552

for comparisons to controls: * $p < 0.003$
for comparisons to patients without ASD: ‡ $p < 0.003$

Table VII: Regression models predicting microstructural variables for the template tract ROI method. Entries for each predictor variable refer to their associated β values in the regression model. Predictors marked “NS” did not improve the adjusted R-squared value when added to the model. p-values refer to the significance of the predictor in the model.

	(constant)	LOG(Age)	Sex	Patients without ASD	Patients with ASD	Patients without ASD x LOG(Age)	Patients with ASD x LOG(Age)	R^2
SLF FA	0.322	0.073*					-0.030*	0.248
SLF MD	8.86E-04	-1.10E-04*		3.14E-05			7.08E-05*	0.444
AF Volume	205.0			159.8				0.066
AF FA	0.375	0.059*		-0.031	-0.069*			0.387
AF MD	9.07E-04	-1.40E-04*		2.87E-05			1.08E-04*	0.530
ILF Volume	524.6	961.3*						0.125
ILF FA	0.268	0.104			0.084		-0.117* ‡	0.501
ILF MD	9.61E-04	-1.35E-04*			-8.05E-05		1.65E-04*	0.502
UF FA	0.282	0.040*	0.015					0.297
UF MD	9.53E-04	-1.13E-04*						0.644
IFOF Volume	-100.5	1247.3*	377.0				-936.4	0.192
IFOF FA	0.338	0.083*						0.416
IFOF MD	1.00E-03	-1.53E-04*						0.276

for comparisons to controls: * $p < 0.003$
for comparisons to patients without ASD: ‡ $p < 0.003$

Table VIII: Regression models predicting microstructural variables for the fractional occupancy method. Entries for each predictor variable refer to their associated β values in the regression model. Predictors marked “NS” did not improve the adjusted R-squared value when added to the model. p-values refer to the significance of the predictor in the model.

	(constant)	β value for DTI predictor	Sex	LOG(Age)	R^2
SLF FA Laterality					
Verbal IQ	71.2	-50.6	31.6*		0.830
Performance - Verbal IQ Split	23.5	-8.2	46.4	-16.1	0.597
SLF FA					
Verbal IQ	27.5	110.6	36.4*		0.833
Performance - Verbal IQ Split					
AF FA Laterality					
Verbal IQ	72.4	-57.8	32.3*		0.834
Performance - Verbal IQ Split	10.2	69.4	-8.5		0.550
AF FA					
Verbal IQ	21.7	128.1	33.4		0.859
Performance - Verbal IQ Split					
AF MD					
Verbal IQ	145.300	-8.43E04	29.3*		0.883
ILF FA Laterality					
Verbal IQ					
Performance - Verbal IQ Split					
ILF FA					
Verbal IQ					
Performance - Verbal IQ Split					

* $p < 0.004$

Table IX: Regression models predicting verbal IQ and performance – verbal IQ split. All microstructural variables were calculated with the template tract ROI method. Entries for each predictor variable refer to their associated β values in the regression model. Predictors marked "NS" did not improve the adjusted R-squared value when added to the model. p-values refer to the significance of the predictor in the model.

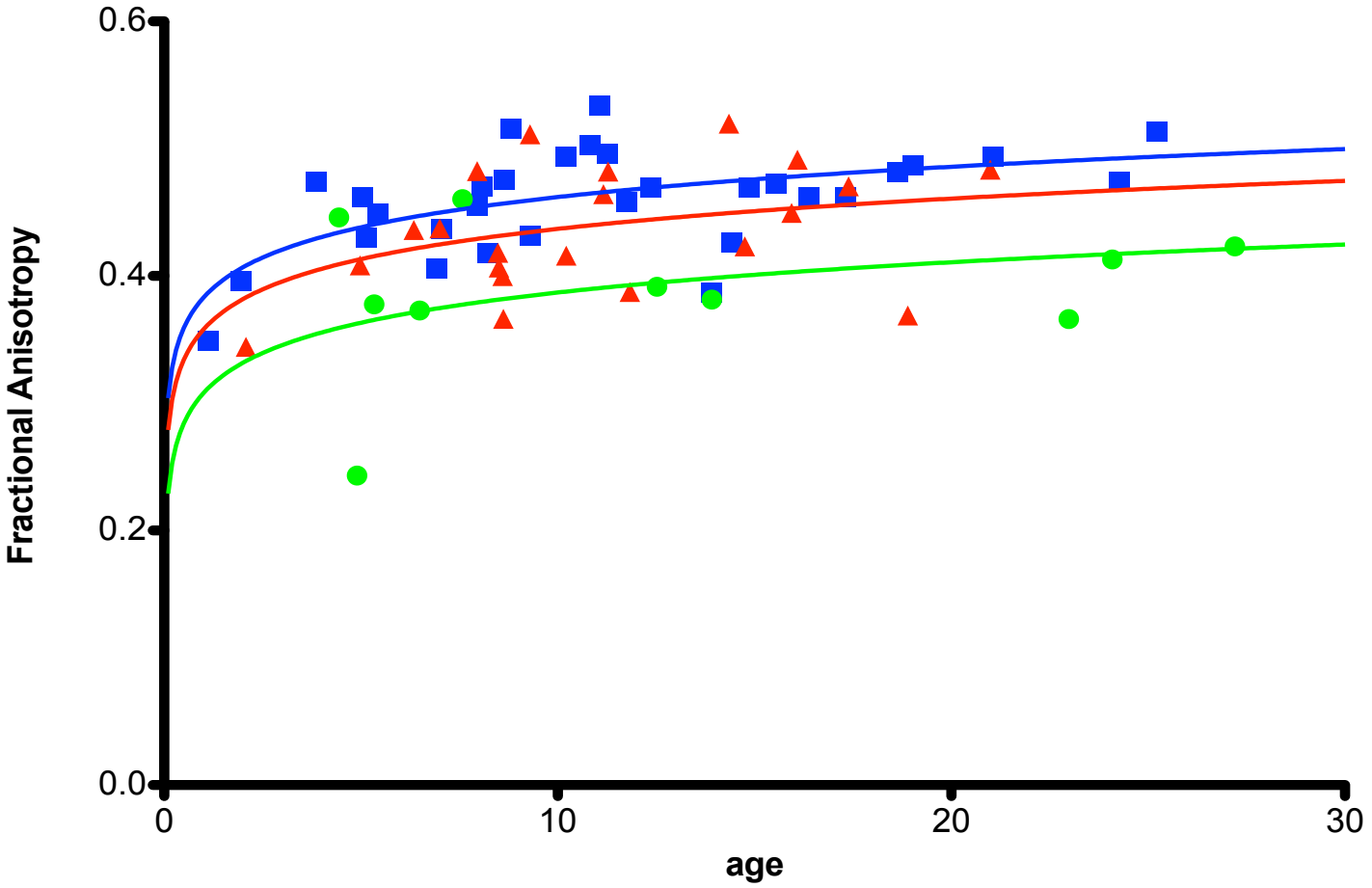

Figure 7: Scatter plot relating AF FA to age. AF FA was calculated with the traditional tractography method. Control subjects are represented by blue squares, TSC patients without ASD by red triangles, and TSC patients with ASD by green circles. The solid lines show the regression model for each group.

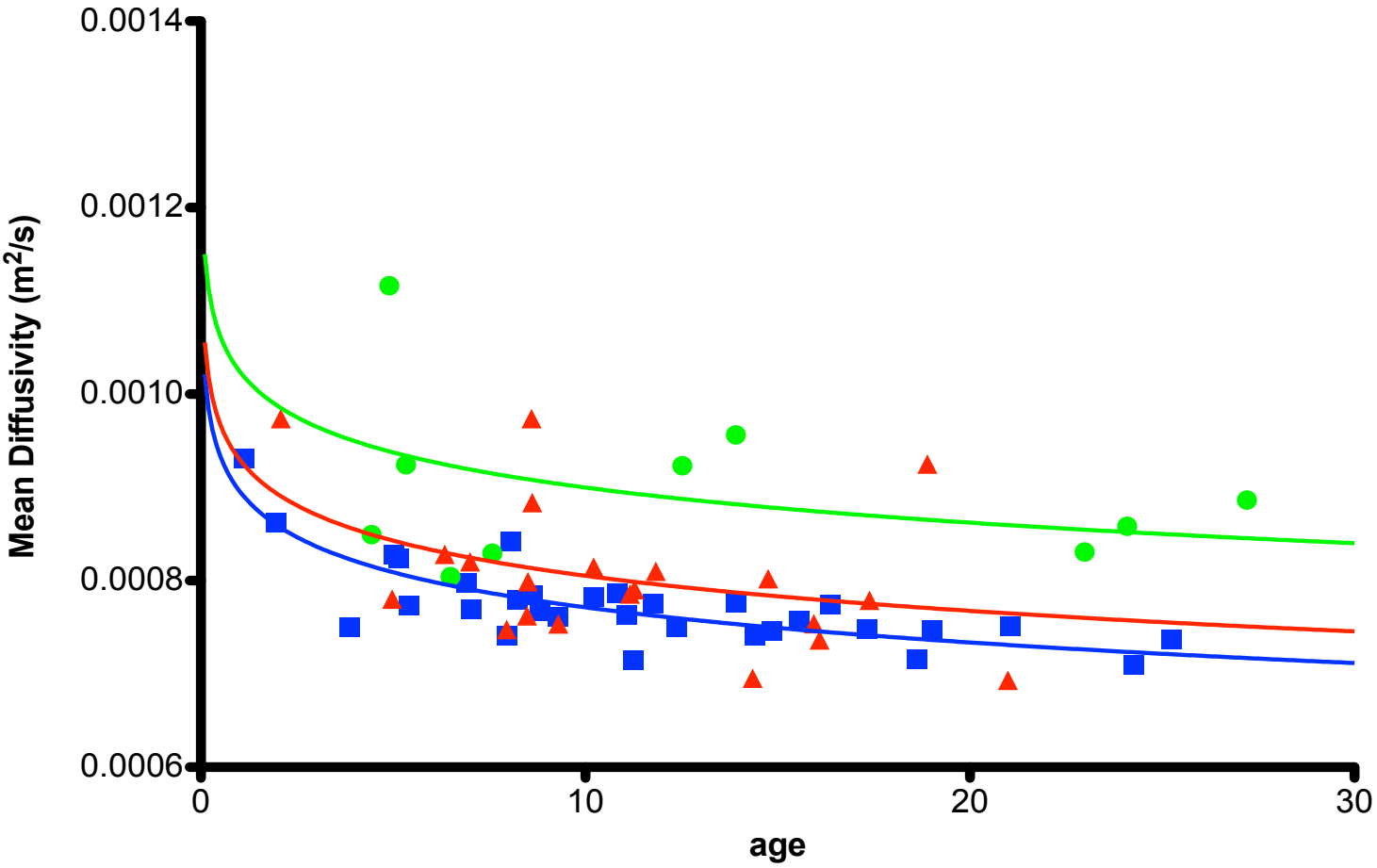

Figure 8: Scatter plot relating AF MD to age. AF MD was calculated with the traditional tractography method. Control subjects are represented by blue squares, TSC patients without ASD by red triangles, and TSC patients with ASD by green circles. The solid lines show the regression model for each group.

ILF FA Laterality

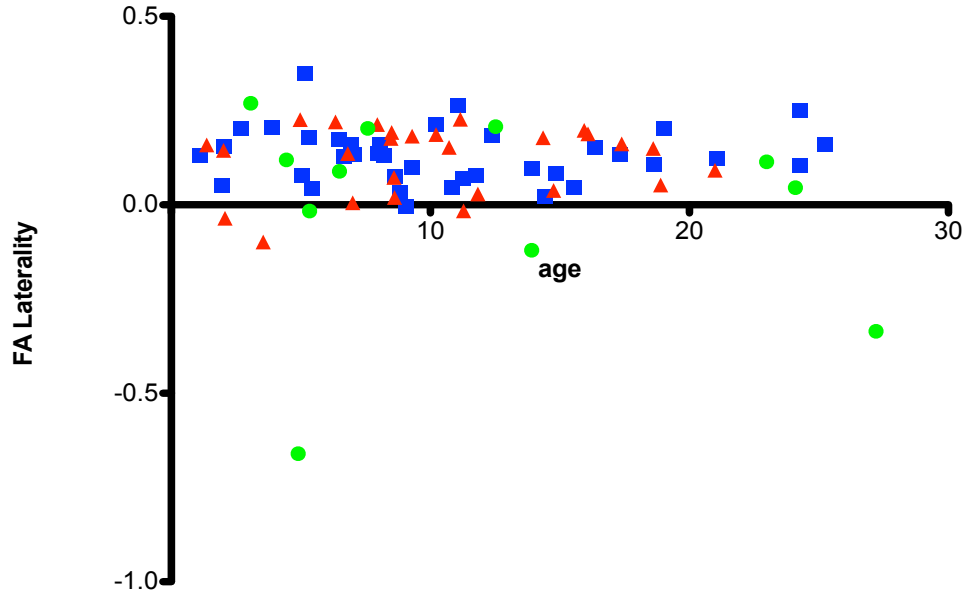

IFOF Volume

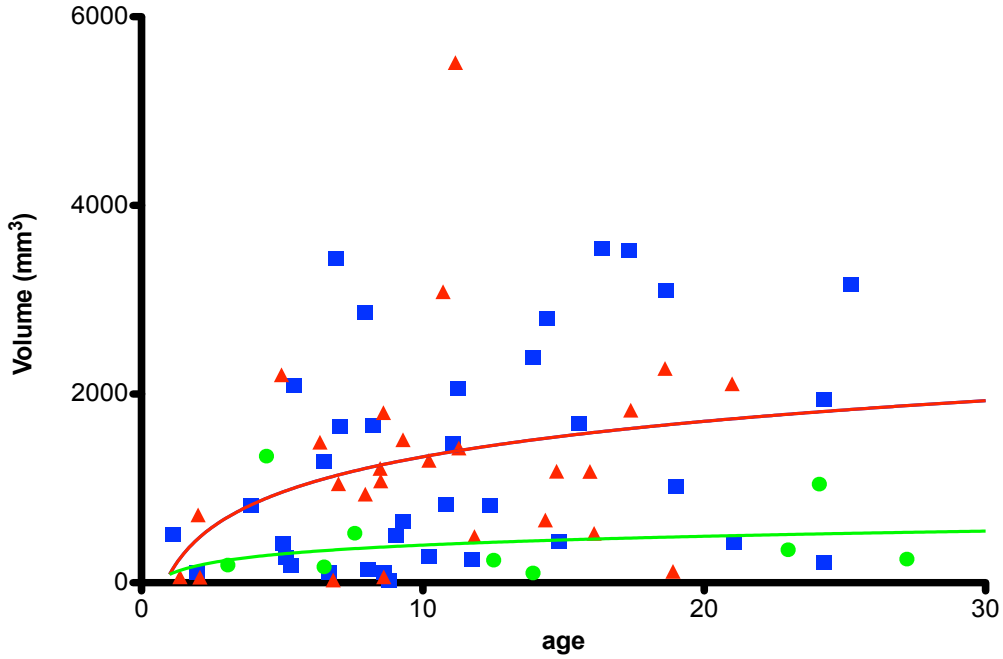

Figure 9: Notable results from the new methods. At the top is ILF FA laterality calculated with the template tract ROI method. Below is the IFOF volume calculated with the fractional occupancy method. Control subjects are represented by blue squares, TSC patients without ASD by red triangles, and TSC patients with ASD by green circles. The solid lines show the regression model for each group.

AF FA:

Traditional Tractography:

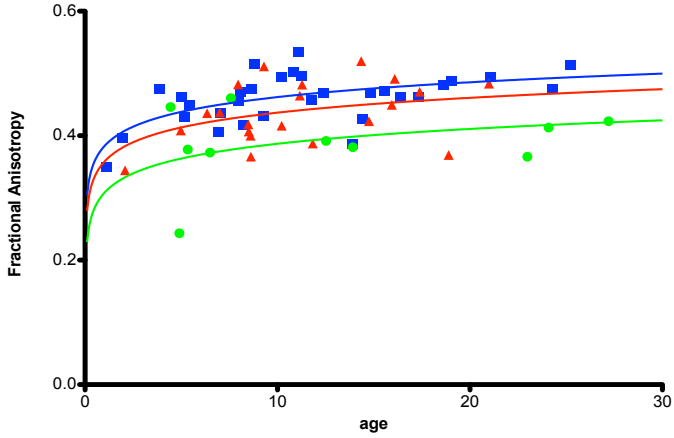

AF MD:

Traditional Tractography:

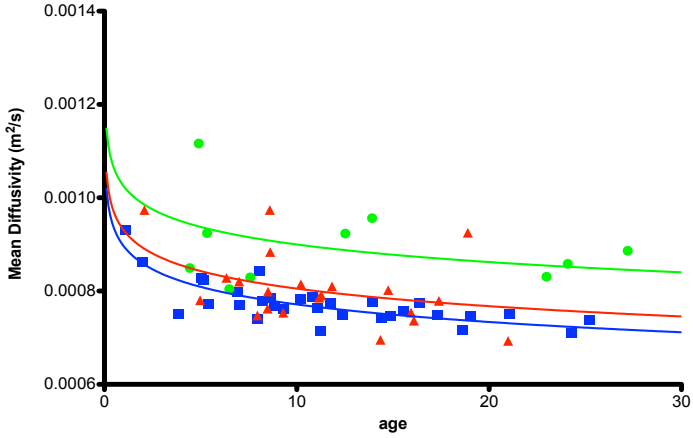

Template Tract ROI:

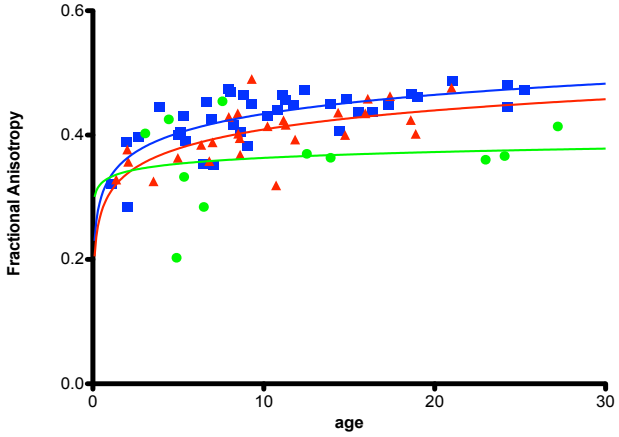

Template Tract ROI:

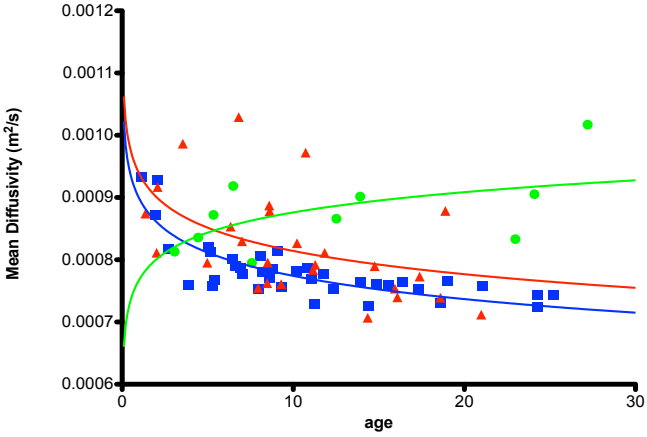

Fractional Occupancy:

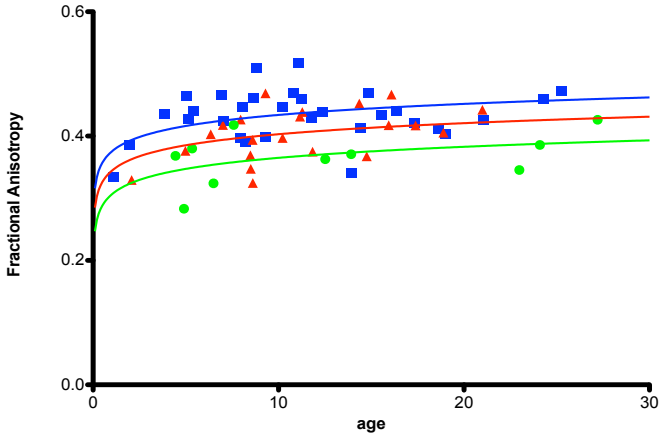

Fractional Occupancy:

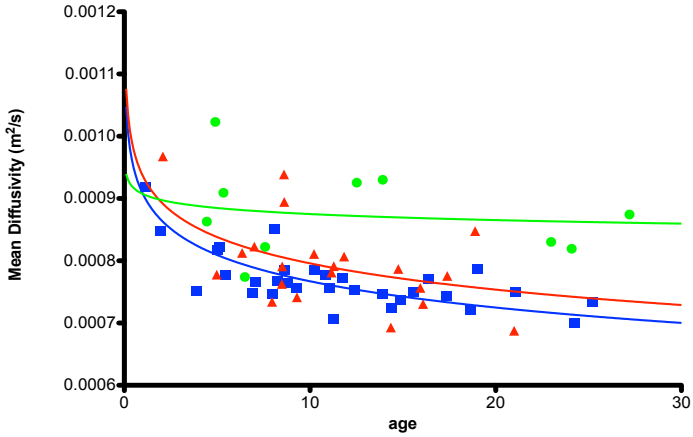

Figure 10: A comparison of the results for AF FA and AF MD with the three methods. Control subjects are represented by blue squares, TSC patients without ASD by red triangles, and TSC patients with ASD by green circles. The solid lines show the regression model for each group.

SLF MD: traditional tractography

Right:

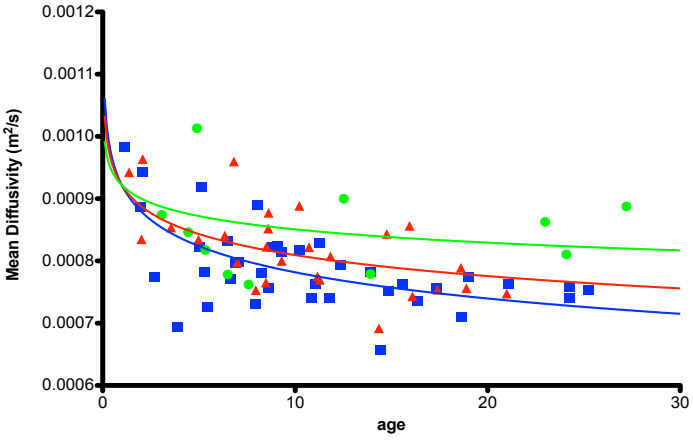

Left:

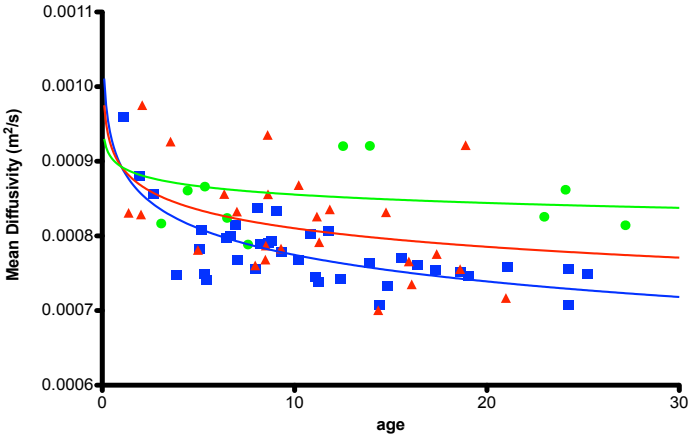

AF MD: template tract ROI

Right:

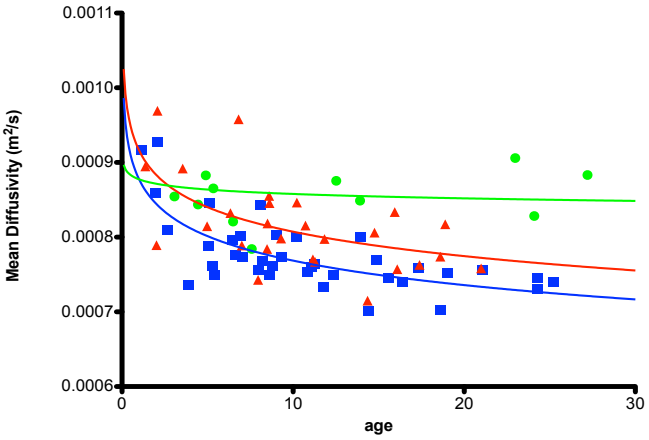

Left:

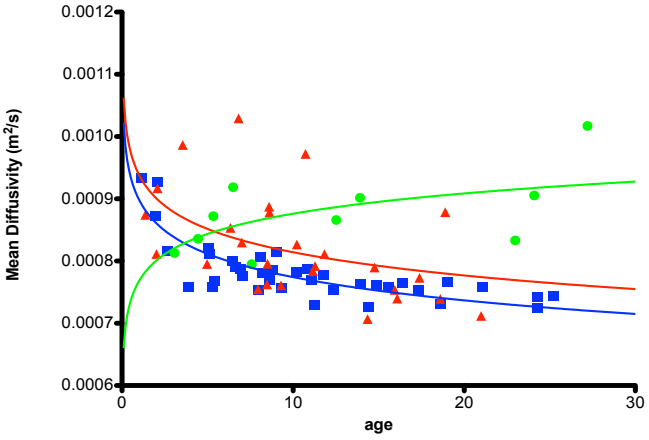

Figure 11: Left vs. right comparison of microstructural values. At left is SLF MD with traditional tractography. At right is AF MD calculated with the template tract ROI method. Control subjects are represented by blue squares, TSC patients without ASD by red triangles, and TSC patients with ASD by green circles. The solid lines show the regression model for each group.

SLF

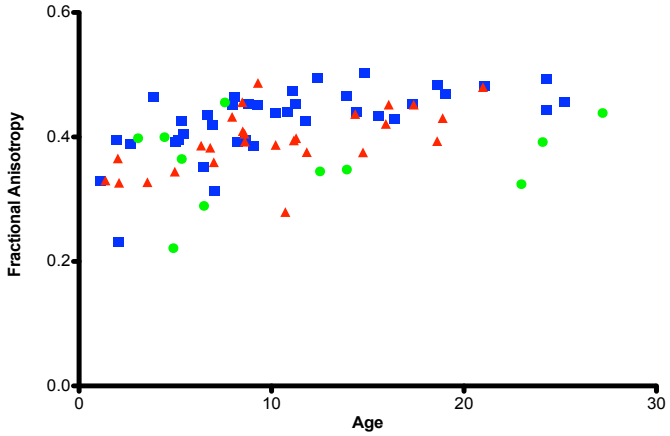

UF

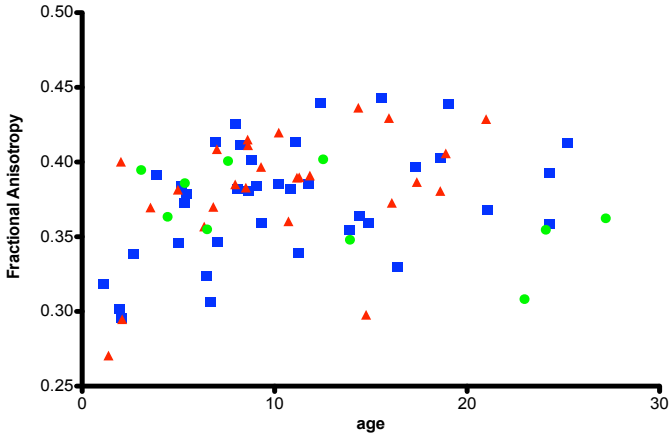

AF

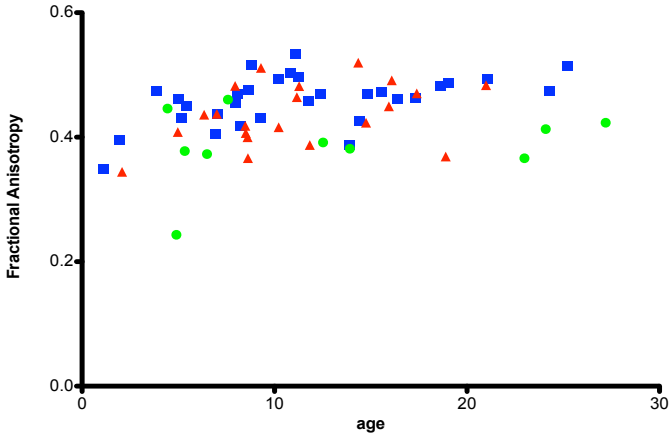

IFOF

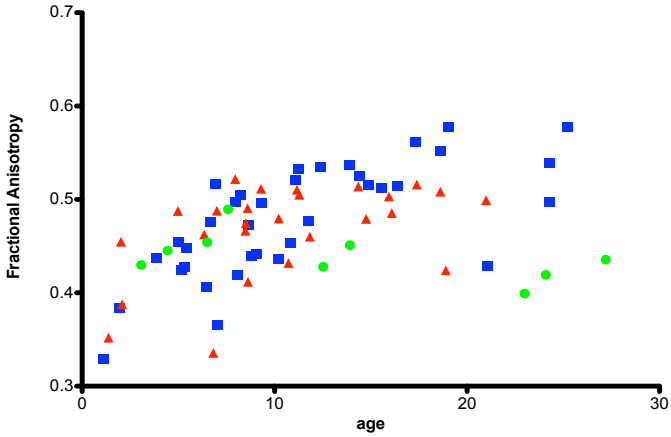

ILF

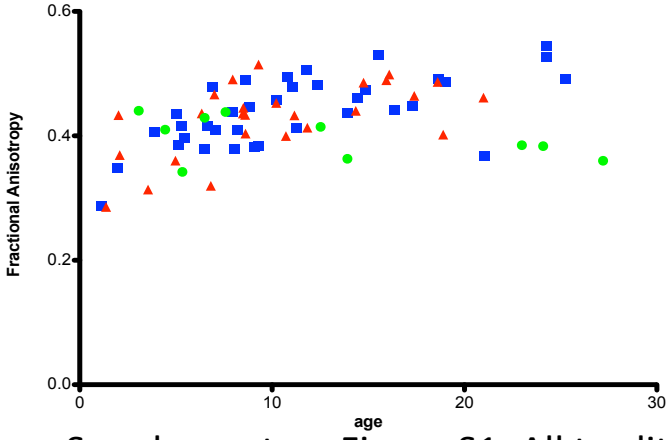

AF for <10

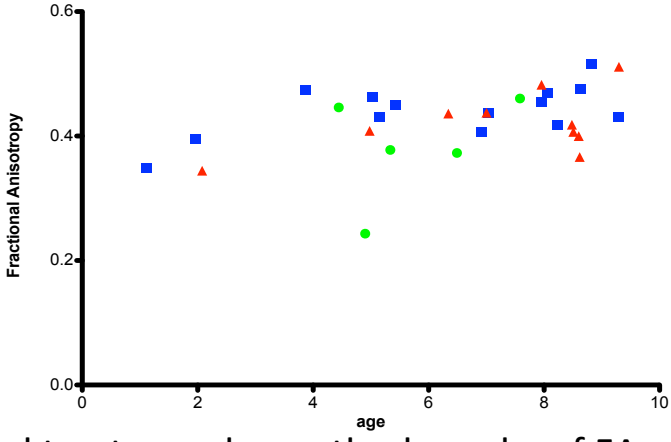

Supplementary Figure S1: All traditional tractography method graphs of FA versus age. AF < 10 is AF data for all subjects younger than 10 years of age. Control subjects are represented by blue squares, TSC patients without ASD by red triangles, and TSC patients with ASD by green circles.

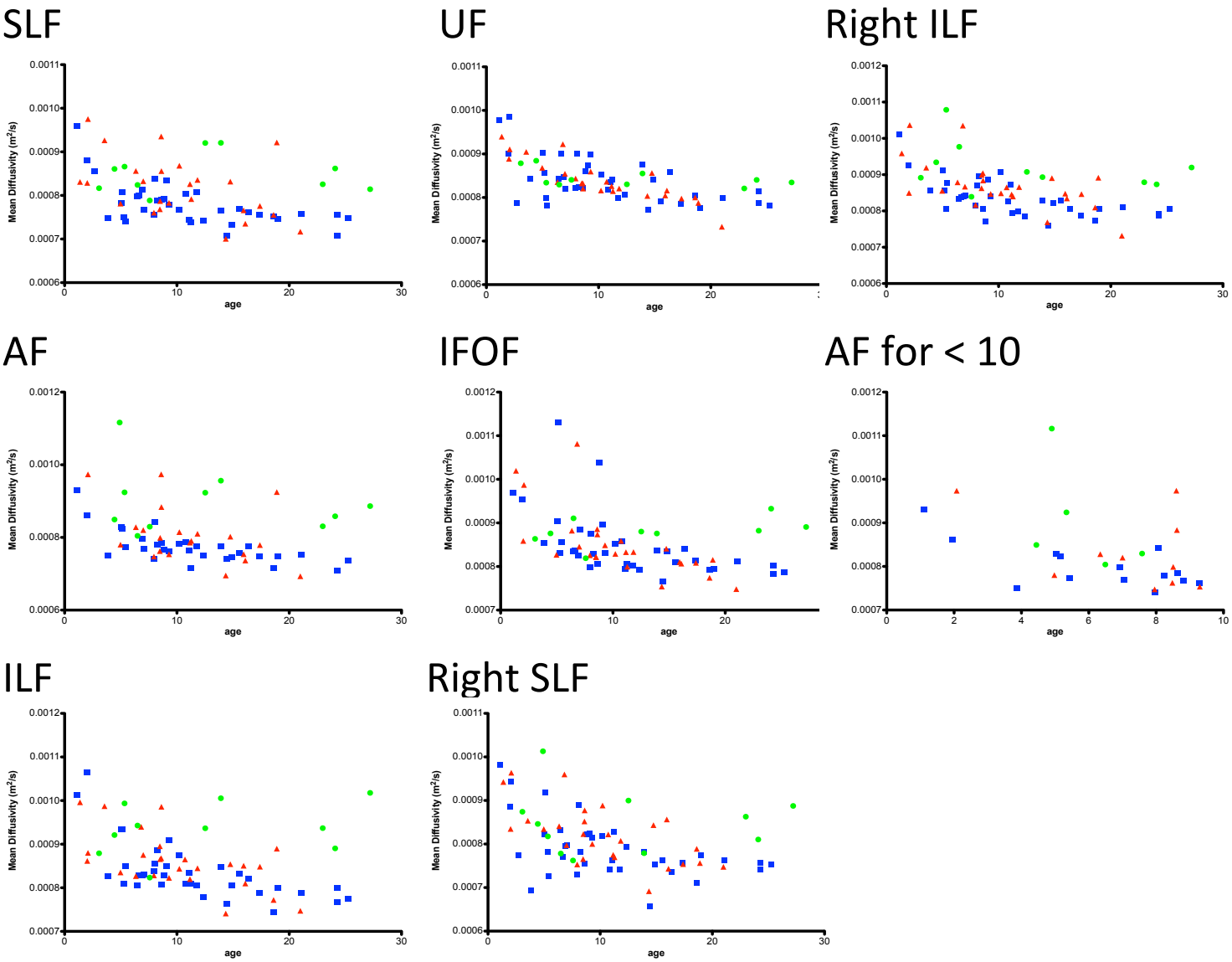

Supplementary Figure S2: All traditional tractography method graphs of MD versus age. AF for < 10 is AF data for all subjects younger than 10 years of age. Control subjects are represented by blue squares, TSC patients without ASD by red triangles, and TSC patients with ASD by green circles.

SLF

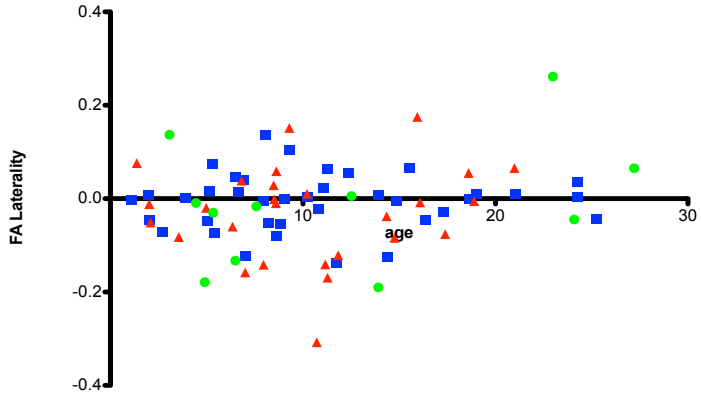

UF

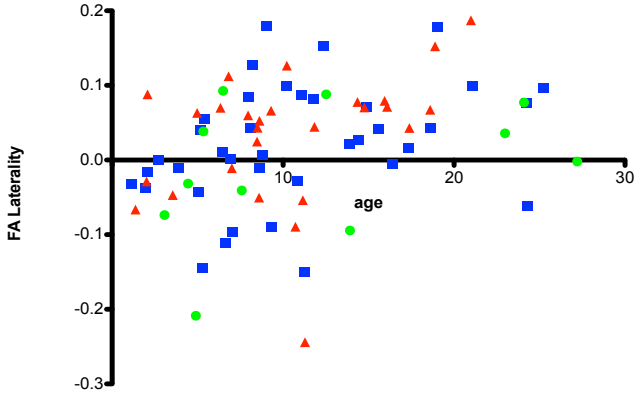

AF

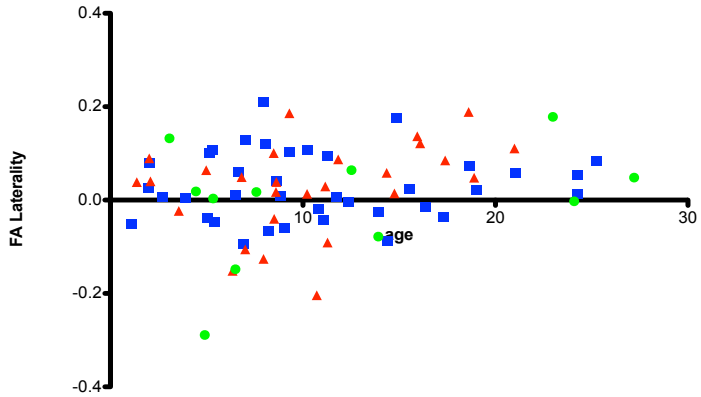

IFOF

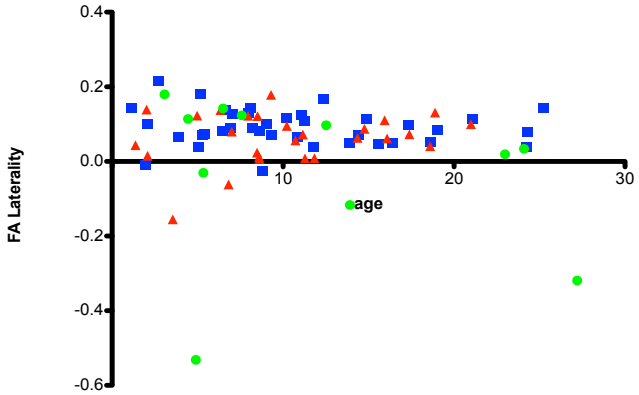

ILF

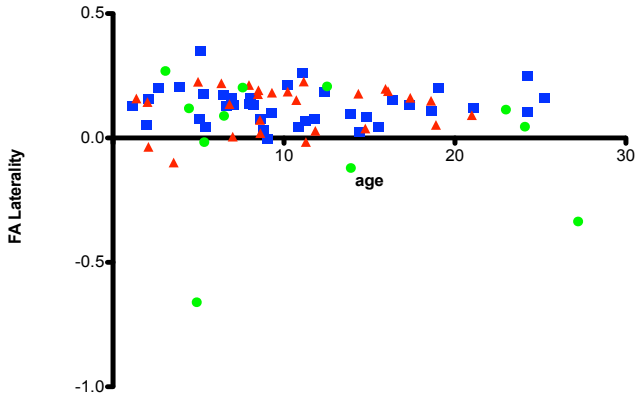

Supplementary Figure S3: All template tract ROI method graphs of FA laterality. Control subjects are represented by blue squares, TSC patients without ASD by red triangles, and TSC patients with ASD by green circles.

SLF

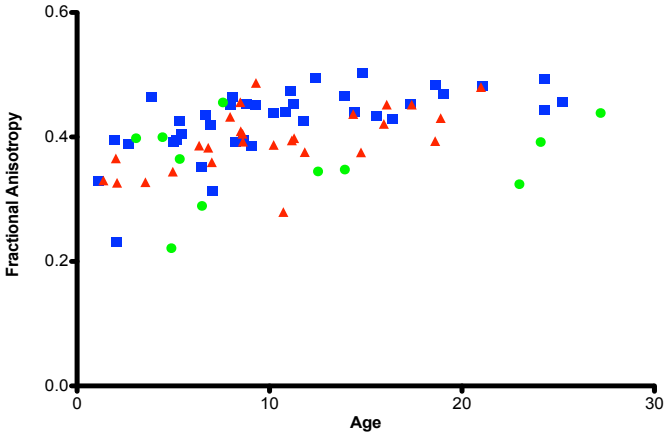

UF

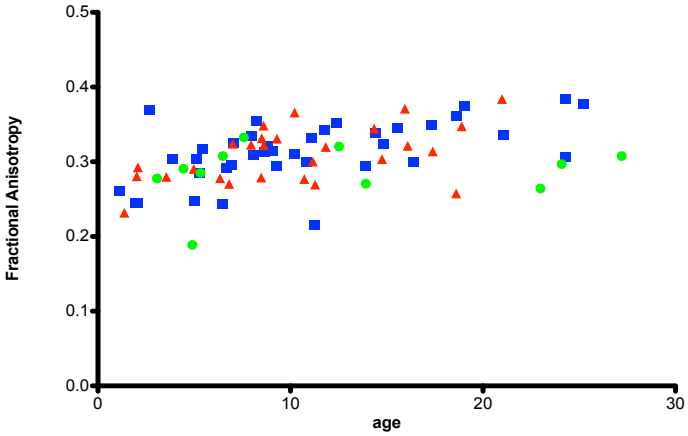

AF

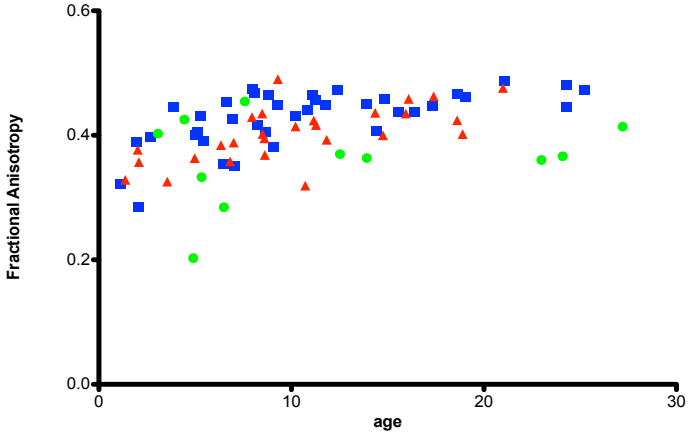

IFOF

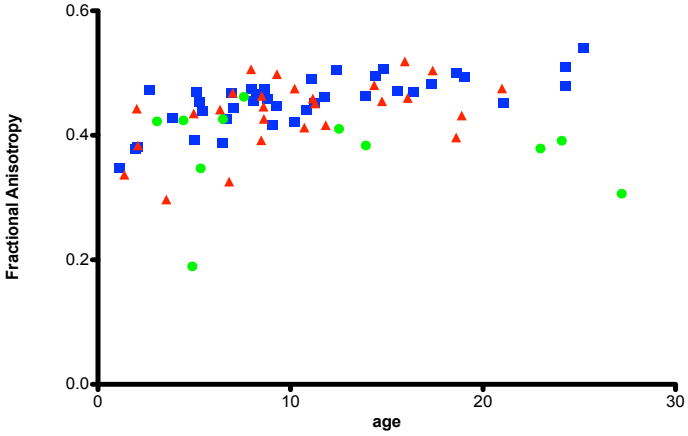

ILF

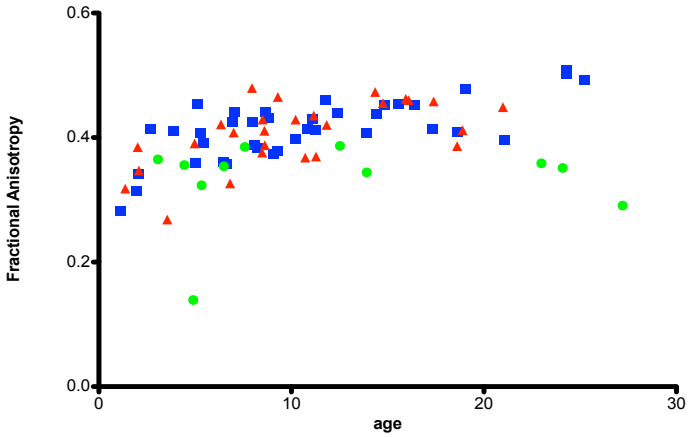

Supplementary Figure S4: All template tract ROI method graphs of FA. Control subjects are represented by blue squares, TSC patients without ASD by red triangles, and TSC patients with ASD by green circles.

SLF

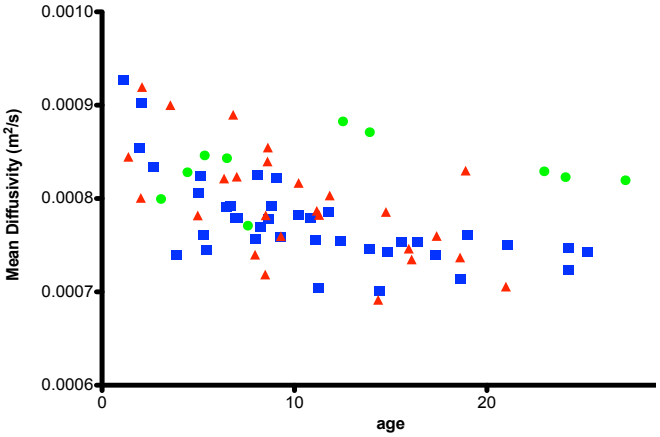

UF

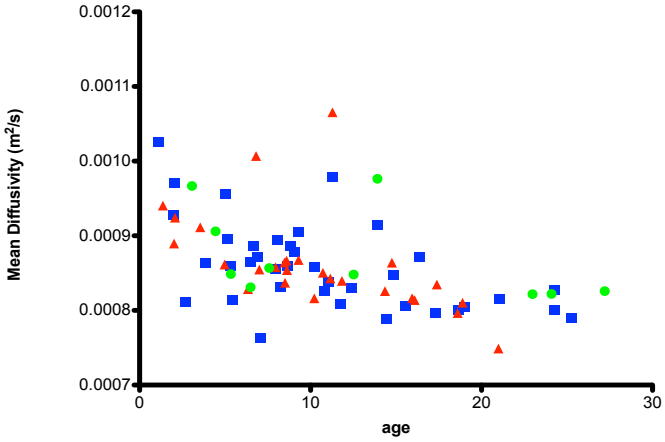

AF

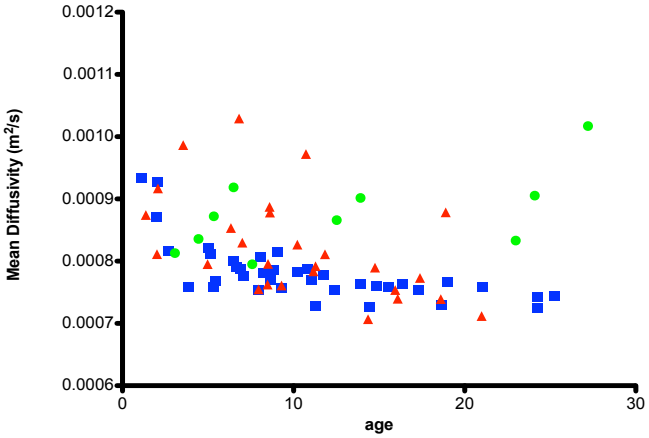

IFOF

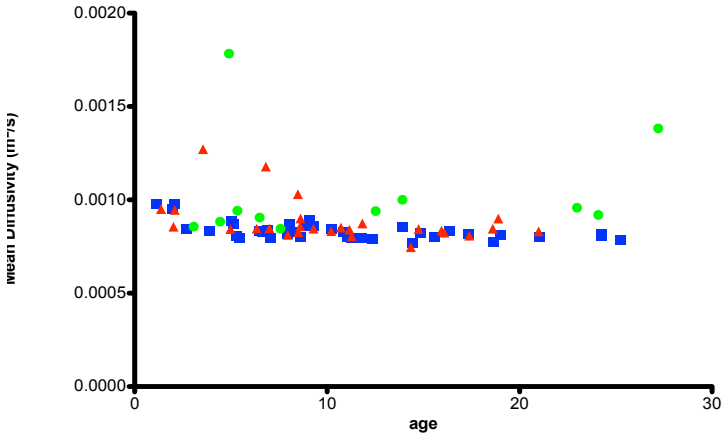

ILF

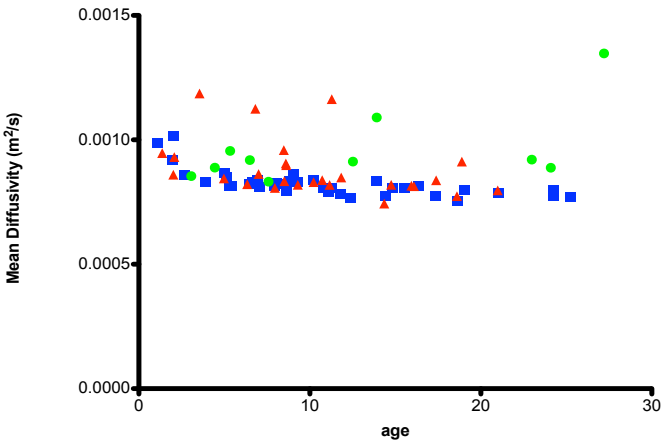

Right AF

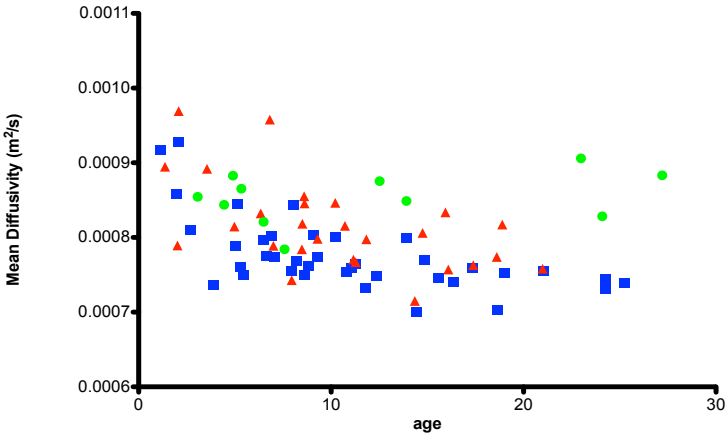

Supplementary Figure S5: All template tract ROI method graphs of MD. Control subjects are represented by blue squares, TSC patients without ASD by red triangles, and TSC patients with ASD by green circles.

SLF

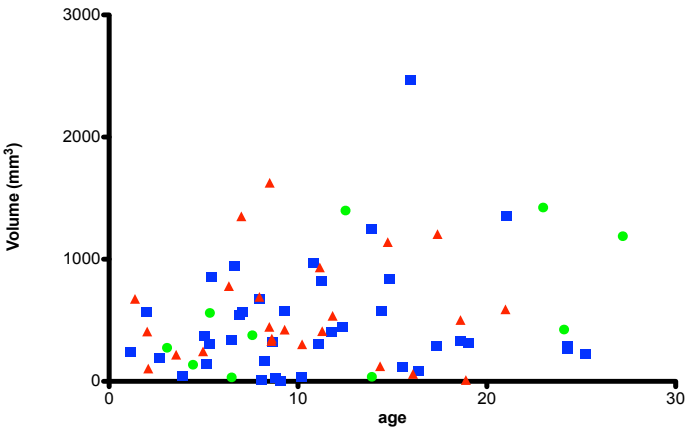

UF

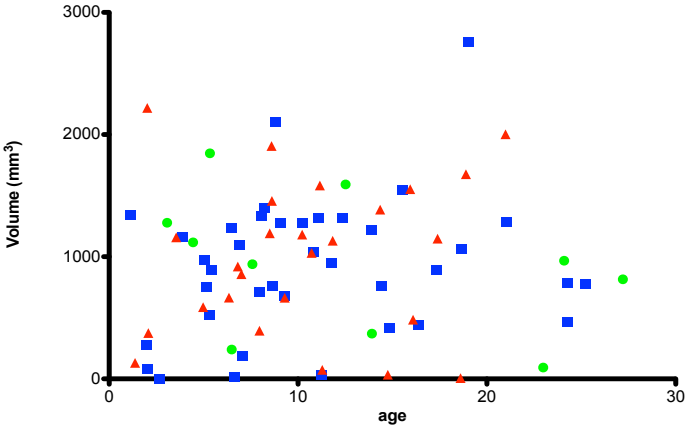

AF

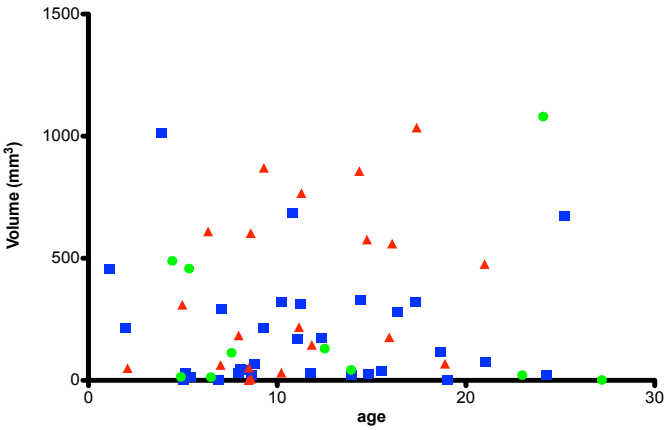

IFOF

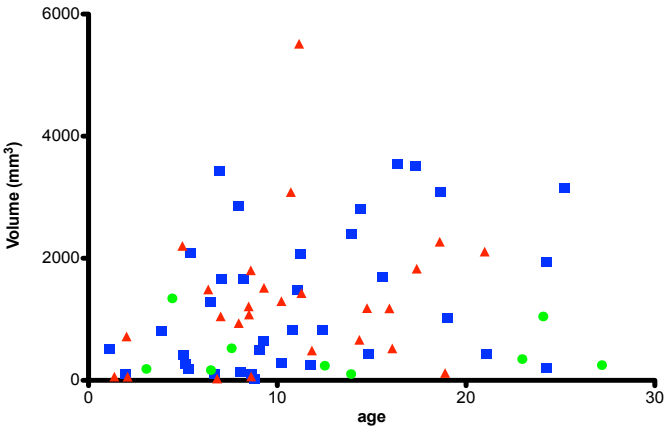

ILF

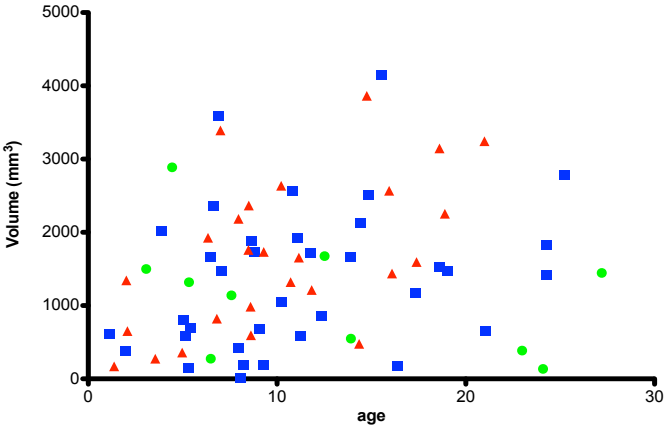

Supplementary Figure S6: All fractional occupancy method graphs of volume. Control subjects are represented by blue squares, TSC patients without ASD by red triangles, and TSC patients with ASD by green circles.

SLF

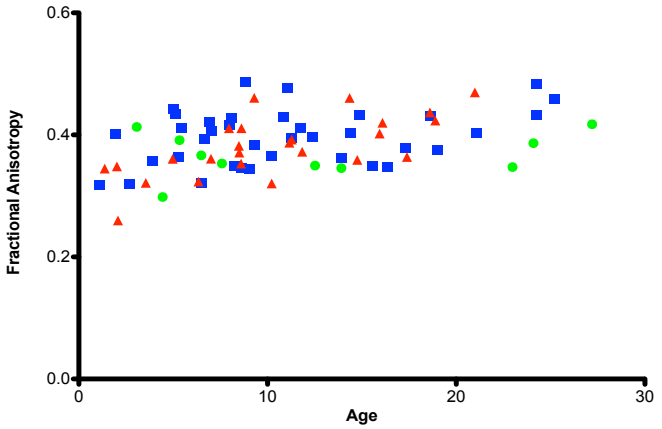

UF

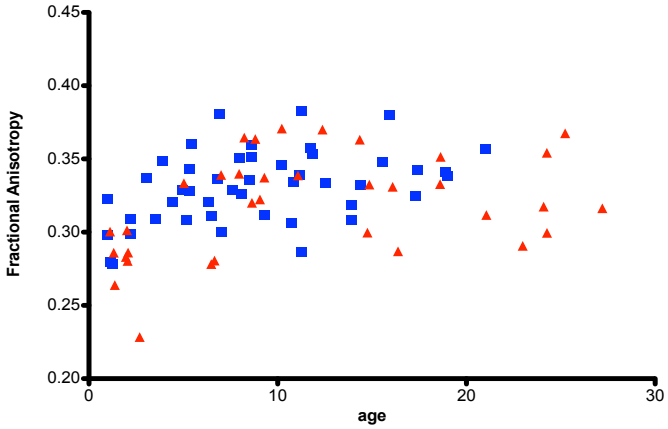

AF

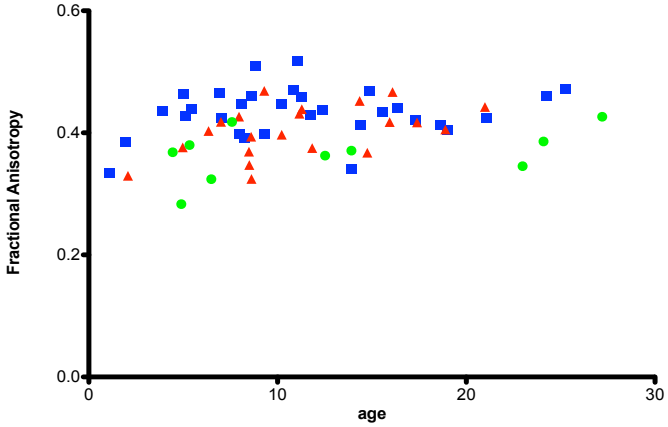

IFOF

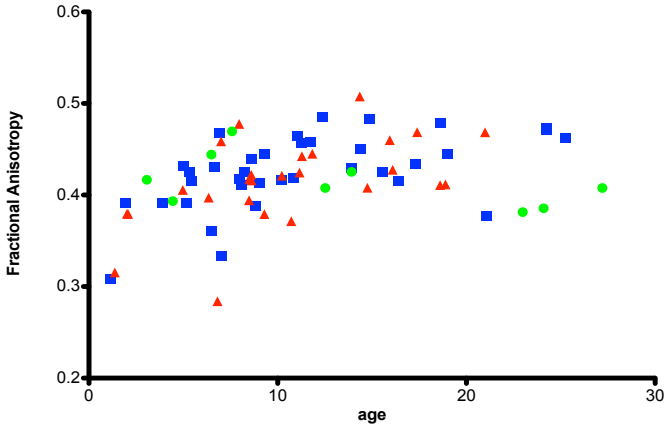

ILF

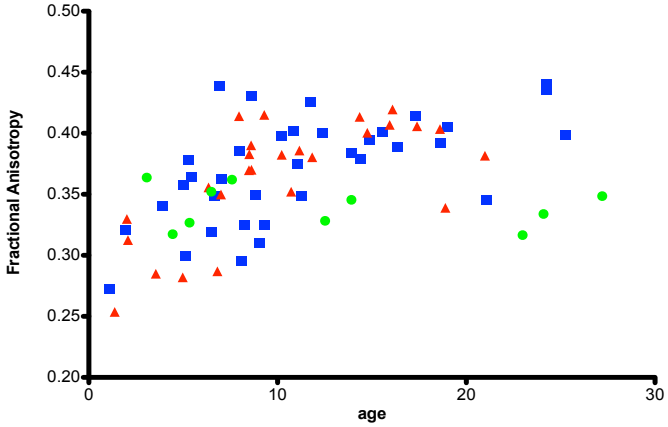

Supplementary Figure S7: All fractional occupancy method graphs of FA. For all except the UF, control subjects are represented by blue squares, TSC patients without ASD by red triangles, and TSC patients with ASD by green circles. For the UF, males are represented by blue squares and females by red triangles.

SLF

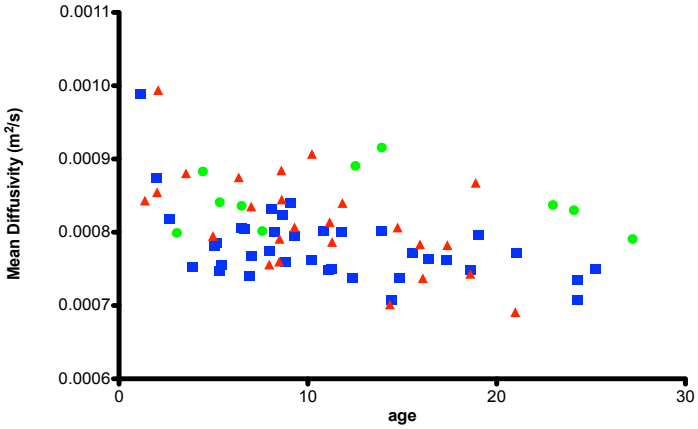

UF

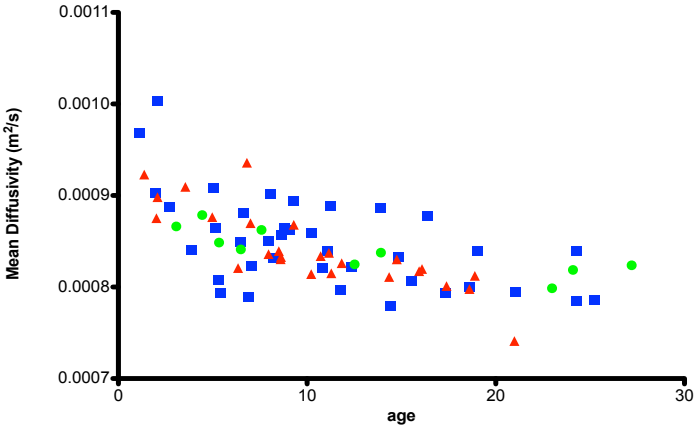

AF

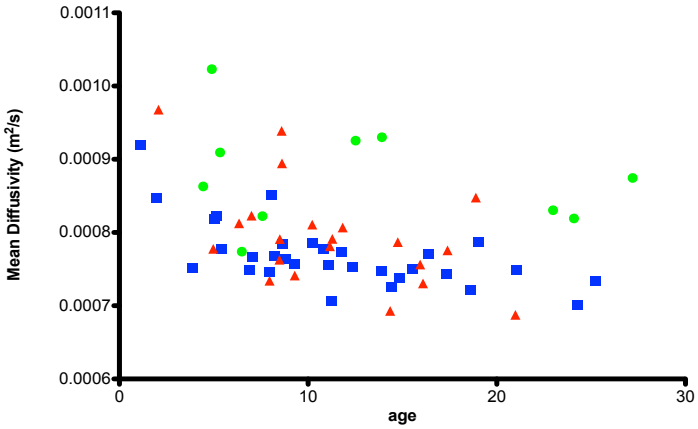

IFOF

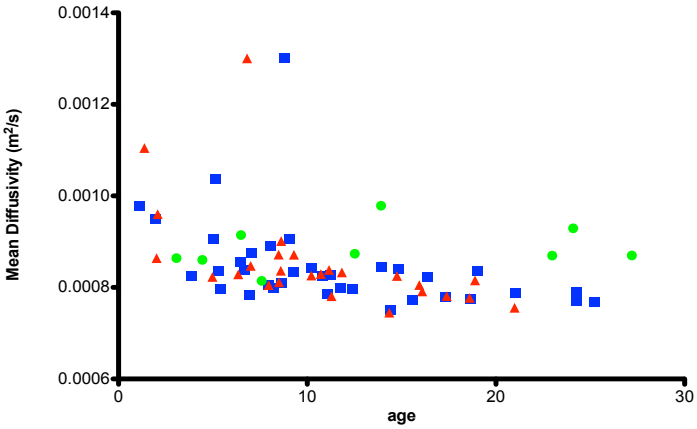

ILF

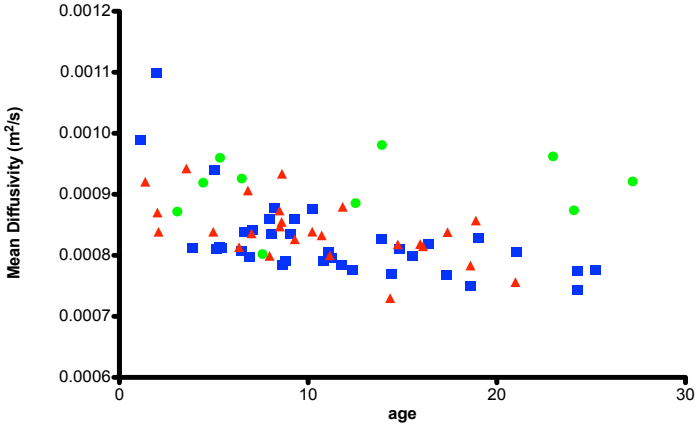

Supplementary Figure S8: All fractional occupancy method graphs of MD. Control subjects are represented by blue squares, TSC patients without ASD by red triangles, and TSC patients with ASD by green circles.